PHYSICAL REVIEW D **86,** 056006 (2012)

New physics effects and hadronic form factor uncertainties in $B \to K^* \ell^+ \ell^-$

Diganta Das and Rahul Sinha

The Institute of Mathematical Sciences, Taramani, Chennai 600113, India

(Received 17 May 2012; published 21 September 2012)

It is well known that new physics can contribute to weak decays of heavy mesons via virtual processes during its decays. The discovery of new physics, using such decays is made difficult due to intractable strong interaction effects needed to describe it. Modes such as $B \to K^* \ell^+ \ell^-$ offer an advantage as they provide a multitude of observables via angular analysis. We show how the multitude of "related observables" obtained from $B \to K^* \ell^+ \ell^-$, can provide many new "clean tests" of the standard model. The hallmark of these tests is that several of them are independent of the unknown universal form factors that describe the decay in heavy quark effective theory. We derive a relation between observables that is free of form factors and Wilson coefficients, the violation of which will be an unambiguous signal of new physics. We also derive relations between observables and form factors that are independent of Wilson coefficients and enable verification of hadronic estimates. We show how form factor ratios can be measured directly from helicity fraction with out any assumptions what so ever. We find that the allowed parameter space for observables is very tightly constrained in standard model, thereby providing clean signals of new physics. We examine in detail both the large-recoil and low-recoil regions of the K^* meson and point out special features and derive relations between observables valid in the two limits. In the large-recoil regions several of the relations are unaffected by corrections to all orders in α_s. We present yet another new relation involving only observables that would verify the validity of the relations between form factors assumed in the low-recoil region. The several relations and constraints derived will provide unambiguous signals of new physics if it contributes to these decays.

DOI: 10.1103/PhysRevD.86.056006 PACS numbers: 11.30.Er, 12.60.−i, 13.25.Hw

I. INTRODUCTION

It is well known that physics beyond the standard model, referred to as new physics, can either be discovered by direct production of new particles at high energies or by indirect searches at high luminosity facilities where new physics can contribute virtually to loop processes. The most well known example of the latter kind is the muon magnetic moment. Unfortunately, even though muon is a lepton, hadronic contributions have to be estimated and turn out to be the limiting factor in the search for new physics. Indirect searches for new physics often involve precision measurement of a single quantity as in the case of muon magnetic moment. The single measurement is compared to a theoretical estimate that needs to be accurately calculated. There are, however, certain decays which involve measurement of several related observables. Well-known examples of such decays are $B \to V_1 V_2$ where B decays to two vector mesons V_1 and V_2 and the semileptonic penguin decay $B \to K^* \ell^+ \ell^-$. The heavy meson decays to such modes occur in multiple partial waves and allow a measurement of a multitude of related observables. In this paper we will show how the observables obtained from an angular analysis of $B \to K^* \ell^+ \ell^-$ allow for a cleaner signals of new physics if it exists.

It is hoped that flavor changing neutral current transitions in $b \to s$ and $b \to d$ will be altered by physics beyond the standard model (SM), and their study would reveal possible signal of new physics (NP) if it exists. However, understanding the hadronic flavor changing neutral current decays requires estimating hadronic effects which cannot be completely accurately done. Experimental data collected by the Belle and *BABAR* collaborations at the B factories, CLEO, Tevatron, and now LHCb seem to indicate that new physics does not show up as large and unambiguous effects in flavor physics. This has bought into focus the need for theoretically cleaner observables, i.e., observables that are relatively free from hadronic uncertainties. In the search for new physics it is, therefore, crucial to effectively separate the effect of new physics from hadronic uncertainties that can contribute to the decay.

One of the modes that is regarded as significant in this attempt is $B \to K^* \ell^+ \ell^-$ an angular analysis of which is known to result in a multitude of observables [1–3], each of which is a function of an invariant dilepton mass q^2. Throughout, our discussions we will neglect the lepton and s-quark masses, ignore the very small CP violation arising within the standard model [1,2], and exclude studying the resonant region in q^2. In this limit, any observable that is chosen may eventually be expressed in terms of six real transversity amplitudes that correspond to the three states of polarizations of K^* and the left or right chirality of the lepton ℓ^-. We can, hence, have at best six independent observables. Several different experiments *BABAR*, Belle, CDF, and LHCb have studied the mode $B \to K^* \ell^+ \ell^-$ [4–10], providing valuable data as a function of the dilepton invariant mass q^2 by studying uniangular distributions.

The partial branching fraction is measured in chosen q^2 bins by preforming a complete angular integration. A study of the angular distribution of the direction of the lepton in an appropriately chosen frame (see Sec. III) has also already been done by all the four experiments to measure the forward-backward asymmetry $A_{\rm FB}$ and the longitudinal polarization fraction F_L, in terms of integrated dilepton invariant mass regions of q^2. CDF and LHCb have, in addition, performed an angular study of the azimuthal angle defined as the angle between the planes formed by the leptons and the decay products of K^*, i.e., K, π. We will show that the $F_\perp$ helicity fraction can be obtained from a uniangular distribution of azimuthal angle. Future experimental studies at LHC-B, Belle II, and Super-B will enable the study this mode with significantly larger statistics and make possible the analysis with multiangular distributions and the measurement of all the observables.

In a recent paper [11] it was shown that the multitude of related observables obtained via an angular analysis in $B \to K^*\ell^+\ell^-$ can provide many "clean tests" of the standard model. The hallmark of these tests is that several of them are independent of the universal form factors $\xi_\parallel$ and $\xi_\perp$ required to describe the decay using heavy quark effective theory (HQET). Indeed, in the large recoil region considered in Ref. [11], these relations are even more interesting as they are unaffected by corrections to all orders in α_s. We will refer to such relations that are independent of universal form factors and are unaffected by corrections to all orders in α_s *as* "clean relations." A variety of relations were derived which included relations between observables and form factors that are independent of Wilson coefficients. Such relations are inherently clean and important as they enable verification of hadronic estimates. We show how form factor ratios can be measured directly from ratios of helicity amplitudes measured at the zero crossings of asymmetries without any assumptions what so ever. Another achievement is the derivation of a relation between observables alone, based entirely on the assumption that the amplitudes have form given by the standard model, but which is nevertheless independent of form factors and Wilson coefficients. This relation would provide an unambiguous test of the standard model relying purely on observables. We also presented a clean expression for the "effective photon vertex" involving the same operator that also contributes to the process $B \to K^*\gamma$. We emphasize that the amplitude for $B \to K^*\gamma$ involves the universal form factor $\xi_\parallel$ and is inherently not clean. It is, hence, somewhat surprising that the same vertex can be expressed independent of the universal form factors in heavy quark effective theory in a way that is valid at order $1/m_b$ to all orders in α_s. While C_9 and C_{10} individually depend on form factors, we find that the expression for the ratio C_9/C_{10} is clean. Based purely on the signs of the form factors and the fact that zero crossing of the forward-backward asymmetry has been observed, we convincingly concluded that the signs of the Wilson coefficients are in agreement with standard model. We found that there exist three sets of equivalent solutions to each of the three Wilson coefficients involving different observables. However, only two of the sets are independent. It was shown that the allowed parameter space for observables is very tightly constrained in the standard model, thereby providing clean signals of new physics.

In this paper we not only derive all the expressions presented in Ref. [11] in detail but also derive several new expression and constraints. We extend the analysis to examine in detail both the large-recoil and low-recoil regions of the K^* meson and probe special features and relations valid in the two limits. We present yet another new relation involving only observables that would verify the validity of the relations between form factors assumed in the low-recoil region. Under this approximation mentioned earlier, we have the six real presumably nonzero amplitudes that are described in terms of eight combinations of form factors and Wilson coefficients. We elaborate in this paper how the six observables can be used to verify the standard model and to distinguish possible new physics contributions from hadronic effects, which in the usual approach, hinder the discovery of new physics. This is made possible by fortunate advances in our understanding of these form factors that permit us to make two reliable inputs in terms of ratios of form factors which are well predicted at order $1/m_b$ to all orders in α_s and are free from universal form factors $\xi_\parallel$ and $\xi_\perp$ in heavy quark effective theory.

In this paper we briefly review the theoretical framework of $B \to K^*\ell^+\ell^-$ in the standard model in Sec. II. In Sec. III we express the differential decay distribution in terms of angular variables and helicity amplitudes. We also define observables that are directly measurable by angular analysis. The helicity amplitudes are expressed in terms of form factors in Sec. IV, where we also set up essential notations used throughout the paper. While most of our analysis is independent of the values of form factors, we do use the various symmetries possible in the heavy quark limit to emphasize the variety of interesting results possible with $B \to K^*\ell^+\ell^-$. In Sec. IV A we discuss the symmetry relations among form factors arising in the large recoil limit of the K^* meson. A similar discussion for the low-recoil limit is presented in Sec. IV B. Our model independent analysis is described in details in Sec. V, where we also derive the bulk of new relations. The results presented in this section are in general valid for all q^2. The large recoil limit is obtained simply by assigning the form factors the expressions or values valid in this limit. The low-recoil limit requires special attention and is discussed in Sec. VI, where we consider special features and derive more new interesting new results. In Sec. VII we summarize the main results of the paper. The derivation involved in the solutions of Wilson coefficients are given in Appendix A, and the numerical values of form factors and inputs we used are presented in Appendix B.

II. THEORETICAL FRAMEWORK

The decay $B(p) \to K^*(k)\ell^-(q_1)\ell^-(q_2)$ is described within the standard model by an effective Hamiltonian $\mathcal{H}_{\rm eff}$ that involves separation of long-distance QCD effects from the short-distance QCD and weak interaction effects. The effective short-distance Hamiltonian for $b \to s\ell^+\ell^-$ transition is well understood and is given by [2,3,12]

$$\mathcal{H}_{\rm eff} = \frac{G_F\alpha}{\sqrt{2}\pi} V_{tb}V_{ts}^*\bigg[C_9^{\rm eff}(\bar{s}\gamma_\mu P_L b)\bar{\ell}\gamma^\mu\ell + C_{10}(\bar{s}\gamma_\mu P_L b)\bar{\ell}\gamma^\mu\gamma_5\ell - \frac{2C_7^{\rm eff}}{q^2}(\bar{s}i\sigma_{\mu\nu}q^\nu m_b P_R b)\bar{\ell}\gamma^\mu\ell\bigg], \quad (1)$$

where $q_\nu = q_{1\nu} + q_{2\nu} = p_\nu - k_\nu$ and we have defined

$$P_{L,R} = \frac{(1 \mp \gamma_5)}{2}$$

and q^2 is the dilepton invariant mass squared. In the above we have ignored the s quark mass and throughout this paper we will ignore the lepton mass. The Wilson coefficients $C_{7,9,10}^{\rm eff}$ are evaluated at the scale $\mu = m_b = 4.8$ GeV at next-to-next-to-leading logarithm accuracy [3]:

$$C_7^{\rm eff} = -0.304, \quad C_9^{\rm eff} = 4.211 + Y(q^2), \quad C_{10} = -4.103,$$

where

$$C_7^{\rm eff} = C_7 - \frac{1}{3}C_3 - \frac{4}{9}C_4 - \frac{20}{3}C_5 - \frac{80}{9}C_6$$

and the function $Y(q^2)$ is given by [3,13–15]

$$\begin{aligned} Y(q^2) = {}& h(q^2, m_c)\left(\frac{4}{3}C_1 + C_2 + 6C_3 + 60C_5\right) \\ & - \frac{1}{2}h(q^2, m_b)\left(7C_3 + \frac{4}{3}C_4 + 76C_5 + \frac{64}{3}C_6\right) \\ & - \frac{1}{2}h(q^2, 0)\left(C_3 + \frac{4}{3}C_4 + 16C_5 + \frac{64}{3}C_6\right) \\ & + \frac{4}{3}C_3 + \frac{64}{9}C_5 + \frac{64}{27}C_6. \end{aligned}$$

The function $h(q^2, m_q)$ reads

$$\begin{aligned} h(q^2, m_q) = {}& -\frac{4}{9}\left(\ln\frac{m_q^2}{\mu^2} - \frac{2}{3} - y\right) - \frac{4}{9}(2 + y) \\ & \times \sqrt{|y - 1|}\bigg[\Theta(1 - y)\left(\ln\frac{1 + \sqrt{1 - y}}{\sqrt{y}} - i\frac{\pi}{2}\right) \\ & + \Theta(y - 1)\arctan\frac{1}{\sqrt{y - 1}}\bigg] \end{aligned}$$

where we have defined $y = 4m_q^2/q^2$, and we have neglected the small weak phase.

The $B \to K^*$ hadronic matrix elements of the local quark bilinear operators $\bar{s}\gamma_\mu P_L b$ and $\bar{s}i\sigma_{\mu\nu}q^\nu m_b P_R b$ can be parametrized in terms of the q^2-dependent QCD form factors V, $A_{1,2}$, $T_{1,2,3}$ as

$$\begin{aligned} &\langle \bar{K}^*(k)|\bar{s}\gamma_\mu(1 - \gamma_5)b|\bar{B}(p)\rangle \\ &= -i\epsilon_\mu(m_B + m_{K^*})A_1(q^2) + p_\mu(\epsilon^*.q)\frac{2A_2(q^2)}{m_B + m_{K^*}} \\ &\quad + i\epsilon_{\mu\nu\rho\sigma}\epsilon^{*\nu}p^\rho k^\sigma\frac{2V(q^2)}{m_B + m_{K^*}} \end{aligned} \quad (2)$$

$$\begin{aligned} &\langle \bar{K}^*(k)|\bar{s}\sigma_{\mu\nu}q^\nu(1 + \gamma_5)b|\bar{B}(p)\rangle \\ &= i\epsilon_{\mu\nu\rho\sigma}\epsilon^{*\nu}p^\rho k^\sigma 2T_1(q^2) + T_2(q^2)[\epsilon_\mu^*(m_B^2 - m_{K^*}^2) \\ &\quad - 2(\epsilon^*.q)p_\mu] - (\epsilon^*.q)q^2\frac{2T_3(q^2)}{m_B^2 - m_{K^*}^2}p_\mu, \end{aligned} \quad (3)$$

where, $q_\nu = p_\nu - k_\nu$. We have dropped terms proportional to q_μ since the terms $q_\mu\bar{\ell}\gamma^\mu\gamma_5\ell$ and $q_\mu\bar{\ell}\gamma^\mu\ell$ do not contribute in the limit of vanishing lepton mass. The form factors have been studied using QCD sum rules on the light cone, QCD factorization in the heavy quark limit, soft-collinear theory, and using operator product expansion that is valid for large dilepton mass $\sqrt{q^2}$. The decay $B \to K^*\ell^+\ell^-$ has the advantage that it can be studied as a function of the dilepton mass or q^2. If one excludes the resonant region and the very small CP violation arising within SM, all the Wilson coefficients and form factors contributing to the decay are real. In this paper as mentioned above we will make both these assumptions.

The complete angular distribution requires the polarization of K^* or a study of the angular distribution of the K^* decay into $K\pi$. This is readily done in the narrow width approximation for the K^* since the decay of $K^* \to K\pi$ is itself well understood in terms of an effective Lagrangian. The resulting matrix elements are described in a model independent approach in terms of three reliably calculable effective Wilson coefficients that represent short-distance contributions and six (in the limit of vanishing lepton mass) $B \to K^*$ form factors. The $B \to K\pi\ell^+\ell^-$ matrix element can, hence, be written as

$$\begin{aligned} \mathcal{M} = {}& \frac{G_F\alpha}{\sqrt{2}\pi}V_{tb}V_{ts}^*\bigg\{\bigg[C_9^{\rm eff}\langle K\pi|\bar{s}\gamma^\mu P_L b|\bar{B}\rangle\bar{l}\gamma_\mu l \\ & + C_{10}\langle K\pi|\bar{s}\gamma^\mu P_L b|\bar{B}\rangle\bar{l}\gamma_\mu\gamma_5 l \\ & - \frac{2C_7 m_b}{q^2}\langle K\pi|\bar{s}i\sigma_{\mu\nu}q^\nu P_R b|\bar{B}\rangle\bar{l}\gamma_\mu l\bigg\}\bigg]. \end{aligned} \quad (4)$$

III. ANGULAR DISTRIBUTION AND OBSERVABLES

The decay $\bar{B}(p) \to K^*(k)\ell^+(q_1)\ell^-(q_1)$ with $K^*(k) \to K(k_1)\pi(k_2)$ on the mass shell, is completely described by four independent kinematic variables. These are the lepton-pair invariant mass squared $q^2 = (q_1 + q_2)^2$, the angle ϕ between the decay planes formed by $\ell^+\ell^-$ and $K\pi$, respectively, and the angles θ_ℓ and θ_K defined as follows: assuming that the K^* has a momentum along the positive z direction in the B rest frame, θ_K is the angle between the K and the $+z$ axis and θ_ℓ is the angle of the ℓ^- with the $+z$ axis. The differential decay distribution of $B \to K^*\ell^+\ell^-$ can be written as

$$\begin{aligned}\frac{d^4\Gamma(B \to K^*\ell^+\ell^-)}{dq^2 d\cos\theta_\ell d\cos\theta_K d\phi} &= I(q^2, \theta_\ell, \theta_K, \phi)\\ &= \frac{9}{32\pi}[I_1^s \sin^2\theta_K + I_1^c\cos^2\theta_K + (I_2^s\sin^2\theta_K + I_2^c\cos^2\theta_K)\cos 2\theta_\ell + I_3\sin^2\theta_K\sin^2\theta_\ell\cos 2\phi\\ &\quad + I_4\sin 2\theta_K\sin 2\theta_\ell\cos\phi + I_5\sin 2\theta_K\sin\theta_\ell\cos\phi + I_6^s\sin^2\theta_K\cos\theta_\ell + I_7\sin 2\theta_K\sin\theta_\ell\sin\phi\\ &\quad + I_8\sin 2\theta_K\sin 2\theta_\ell\sin\phi + I_9\sin^2\theta_K\sin^2\theta_\ell\sin 2\phi]. \end{aligned}\tag{5}$$

We note that I's are q^2 dependent but we have chosen to suppress the explicit q^2 dependence for simplicity. Throughout the paper, we will not explicitly state the q^2 dependence of observables and variables; however, the dependence is implicit. A study of the angular distribution of the decay will allow us to measures all the I's. Since the K^* in $B \to K^*\ell^+\ell^-$ decay is created on shell, it has three polarization states. Hence, we can express I's explicitly in terms of the six transversity amplitudes $\mathcal{A}^{L,R}_{\perp,\|,0}$, where $\perp$, $\|$, and 0 represent the polarizations and L, R denote the chirality of the lepton ℓ^-. We can write the nine observables explicitly in terms of the six transversity amplitudes $\mathcal{A}^{L,R}_{\perp,\|,0}$ as

$$I_1^s = \frac{3}{4}[|\mathcal{A}_\perp^L|^2 + |\mathcal{A}_\|^L|^2 + (L \to R)], \qquad I_1^c = [|\mathcal{A}_0^L|^2 + (L \to R)], \qquad I_2^s = \frac{1}{4}[|\mathcal{A}_\perp^L|^2 + |\mathcal{A}_\|^L|^2 + (L \to R)],$$

$$I_2^c = -[|\mathcal{A}_0^L|^2 + (L \to R)], \qquad I_3 = \frac{1}{2}[|\mathcal{A}_\perp^L|^2 - |\mathcal{A}_\|^L|^2 + (L \to R)], \qquad I_4 = \frac{1}{\sqrt{2}}[\mathrm{Re}(\mathcal{A}_0^L\mathcal{A}_\|^{L*}) + (L \to R)],$$

$$I_5 = \sqrt{2}[\mathrm{Re}(\mathcal{A}_0^L\mathcal{A}_\perp^{L*}) - (L \to R)], \qquad I_6^s = 2[\mathrm{Re}(\mathcal{A}_\|^L\mathcal{A}_\perp^{L*}) - (L \to R)], \qquad I_7 = \sqrt{2}[\mathrm{Im}(\mathcal{A}_0^L\mathcal{A}_\|^{L*}) - (L \to R)],$$

$$I_8 = \frac{1}{\sqrt{2}}[\mathrm{Im}(\mathcal{A}_0^L\mathcal{A}_\perp^{L*}) + (L \to R)], \qquad I_9 = [\mathrm{Im}(\mathcal{A}_\|^{L*}\mathcal{A}_\perp^L) + (L \to R)].$$

In the above we have ignored the lepton mass. As mentioned above we will assume that the resonant region is excluded in the analysis and that CP violation arising within the standard model is negligible. In the absence of CP violation the conjugate mode $\bar{B} \to \bar{K}^*\ell^+\ell^-$ has an identical decay distribution except that $I_{5,6,8,9}$ switch signs to become $-I_{5,6,8,9}$ in the differential decay distribution [1,2]. The helicity amplitudes $\mathcal{A}^{L,R}_{\perp,\|,0}$ are then all real and only six of the I's can be nonzero and independent. In fact, it is easy to see that I_7, I_8, and I_9 must vanish in the limit of vanishing CP violation.

The explicit form of these transversity amplitudes are

$$\mathcal{A}_\perp^{L,R} = N\sqrt{2}\sqrt{\lambda(m_B^2, m_{K^*}^2, q^2)}\left[[(C_9^{\mathrm{eff}} \mp C_{10}^{\mathrm{eff}})]\frac{V(q^2)}{m_B + m_{K^*}} + \frac{2m_b}{q^2}C_7^{\mathrm{eff}}T_1(q^2)\right], \tag{6a}$$

$$\mathcal{A}_\|^{L,R} = -N\sqrt{2}(m_B^2 - m_{K^*}^2)\left[[(C_9^{\mathrm{eff}} \mp C_{10}^{\mathrm{eff}})]\frac{A_1(q^2)}{m_B - m_{K^*}} + \frac{2m_b}{q^2}C_7^{\mathrm{eff}}T_2(q^2)\right], \tag{6b}$$

$$\begin{aligned}\mathcal{A}_0^{L,R} = -\frac{N}{2m_{K^*}\sqrt{q^2}}\Bigg([(C_9^{\mathrm{eff}} \mp C_{10}^{\mathrm{eff}})] \times \left[(m_B^2 - m_{K^*}^2 - q^2)(m_B + m_{K^*})A_1(q^2) - \lambda(m_B^2, m_{K^*}^2, q^2)\frac{A_2(q^2)}{m_B + m_{K^*}}\right]\\ + 2m_b C_7^{\mathrm{eff}}\left[(m_B^2 + 3m_{K^*}^2 - q^2)T_2(q^2) - \frac{\lambda(m_B^2, m_{K^*}^2, q^2)}{m_B^2 - m_{K^*}^2}T_3(q^2)\right]\Bigg)\end{aligned} \tag{6c}$$

where

$$N = V_{tb}V_{ts}^{*}\left[\frac{G_F^2\alpha^2}{3\cdot 2^{10}\pi^5 m_B^3}q^2\sqrt{\lambda(m_B^2, m_{K^*}^2, q^2)}\right]^{1/2}, \tag{7}$$

with $\lambda(m_B^2, m_{K^*}^2, q^2) = m_B^4 + m_{K^*}^4 + q^4 - 2(m_B^2 m_{K^*}^2 + m_{K^*}^2 q^2 + m_B^2 q^2)$. We note that the helicity amplitudes $\mathcal{A}_{\perp,\|,0}^{L,R}$ are functions of q^2; for simplicity, we have suppressed the explicit dependence on q^2:

$$\begin{aligned} I(q^2,\theta_\ell,\theta_K,\phi) = \frac{9}{16\pi}\Bigg[&\frac{(|\mathcal{A}_\perp^L|^2+|\mathcal{A}_\perp^R|^2+|\mathcal{A}_\|^L|^2+|\mathcal{A}_\|^R|^2)}{4}\sin^2\theta_K(1+\cos^2\theta_\ell)+(|\mathcal{A}_0^L|^2+|\mathcal{A}_0^R|^2)\cos^2\theta_K\sin^2\theta_\ell \\ &+\frac{(|\mathcal{A}_\perp^L|^2+|\mathcal{A}_\perp^R|^2-|\mathcal{A}_\|^L|^2-|\mathcal{A}_\|^R|^2)}{4}\cos 2\phi\sin^2\theta_K\sin^2\theta_\ell+\mathrm{Re}(\mathcal{A}_\|^L\mathcal{A}_\perp^{L*}-\mathcal{A}_\|^R\mathcal{A}_\perp^{R*})\cos\theta_\ell\sin^2\theta_K \\ &+\frac{\mathrm{Re}(\mathcal{A}_0^L\mathcal{A}_\perp^{L*}-\mathcal{A}_0^R\mathcal{A}_\perp^{R*})}{\sqrt{2}}\cos\phi\sin\theta_\ell\sin(2\theta_K)+\frac{\mathrm{Re}(\mathcal{A}_0^L\mathcal{A}_\|^{L*}+\mathcal{A}_0^R\mathcal{A}_\|^{R*})}{2\sqrt{2}}\cos\phi\sin(2\theta_\ell)\sin(2\theta_K)\Bigg]. \end{aligned} \tag{8}$$

It is easy to see that integration over $\cos\theta_K$, $\cos\theta_\ell$, and ϕ results in the differential decay rate with respect to the invariant lepton mass, which is given by the sum of the modulus squared of all the transversity amplitudes at the same invariant lepton mass:

$$\frac{d\Gamma}{dq^2} = \sum_{\lambda=0,\|,\perp}(|\mathcal{A}_\lambda^L|^2+|\mathcal{A}_\lambda^R|^2). \tag{9}$$

It is obvious from Eq. (8) that a complete study of the angular distribution will allow us to measure six observables. We define the relevant observables to be the three helicity fractions defined as follows:

$$F_L = \frac{|\mathcal{A}_0^L|^2+|\mathcal{A}_0^R|^2}{\Gamma_f}, \tag{10a}$$

$$F_\| = \frac{|\mathcal{A}_\|^L|^2+|\mathcal{A}_\|^R|^2}{\Gamma_f}, \tag{10b}$$

$$F_\perp = \frac{|\mathcal{A}_\perp^L|^2+|\mathcal{A}_\perp^R|^2}{\Gamma_f}, \tag{10c}$$

where $\Gamma_f \equiv \sum_\lambda(|\mathcal{A}_\lambda^L|^2+|\mathcal{A}_\lambda^R|^2)$, and $F_L+F_\|+F_\perp=1$. The well-known forward-backward asymmetry A_{FB},

$$A_{\mathrm{FB}} = \frac{[\int_0^1-\int_{-1}^0]d\cos\theta_\ell\frac{d^2(\Gamma+\bar{\Gamma})}{dq^2 d\cos\theta_\ell}}{\int_{-1}^1 d\cos\theta_\ell\frac{d^2(\Gamma+\bar{\Gamma})}{dq^2 d\cos\theta_\ell}}, \tag{11}$$

and two new angular asymmetries,

$$A_4 = \frac{[\int_{\pi/2}^{3\pi/2}d\phi-\int_{-\pi/2}^{\pi/2}d\phi][\int_0^1 d\cos\theta_K-\int_{-1}^0 d\cos\theta_K][\int_0^1 d\cos\theta_\ell-\int_{-1}^0 d\cos\theta_\ell]\frac{d^4(\Gamma-\bar{\Gamma})}{dq^2 d\cos\theta_\ell d\cos\theta_K d\phi}}{\int_0^{2\pi}d\phi\int_{-1}^1 d\cos\theta_K\int_{-1}^1 d\cos\theta_\ell\frac{d^4(\Gamma+\bar{\Gamma})}{dq^2 d\cos\theta_\ell d\cos\theta_K d\phi}}, \tag{12}$$

$$A_5 = \frac{\int_{-1}^1 d\cos\theta_\ell[\int_{\pi/2}^{3\pi/2}d\phi-\int_{-\pi/2}^{\pi/2}d\phi][\int_0^1 d\cos\theta_K-\int_{-1}^0 d\cos\theta_K]\frac{d^4(\Gamma+\bar{\Gamma})}{dq^2 d\cos\theta_\ell d\cos\theta_K d\phi}}{\int_{-1}^1 d\cos\theta_\ell\int_0^{2\pi}d\phi\int_{-1}^1 d\cos\theta_K\frac{d^4(\Gamma+\bar{\Gamma})}{dq^2 d\cos\theta_\ell d\cos\theta_K d\phi}}. \tag{13}$$

A_{FB}, A_4, and A_5 can be written directly in terms of the transversity amplitudes as follows:

$$A_4 = \frac{\sqrt{2}}{\pi}\frac{\mathrm{Re}(\mathcal{A}_0^L\mathcal{A}_\|^{L*})+\mathrm{Re}(\mathcal{A}_0^R\mathcal{A}_\|^{R*})}{\Gamma_f}, \tag{14}$$

$$A_5 = \frac{3}{2\sqrt{2}} \frac{\mathrm{Re}(\mathcal{A}_0^L \mathcal{A}_\perp^{L*} - \mathcal{A}_0^R \mathcal{A}_\perp^{R*})}{\Gamma_f}, \tag{15}$$

$$A_{\mathrm{FB}} = \frac{3}{2} \frac{\mathrm{Re}(\mathcal{A}_\parallel^L \mathcal{A}_\perp^{L*} - \mathcal{A}_\parallel^R \mathcal{A}_\perp^{R*})}{\Gamma_f}. \tag{16}$$

A complete angular analysis requires much larger data set than are currently analyzed, hence, angular distributions in terms of only one angular variable have been studied. The angular distribution as a function of q^2 and $\cos\theta_\ell$ with ϕ and $\cos\theta_K$ integrated out is given by

$$\frac{d^2\Gamma}{dq^2 d\cos\theta_\ell} = \Gamma\Big[A_{\mathrm{FB}}\cos\theta_\ell + \frac{3}{8}(1 - F_L)(1 + \cos^2\theta_\ell) + \frac{3}{4}F_L(1 - \cos^2\theta_\ell)\Big]. \tag{17}$$

Angular analysis in terms of $\cos\theta_\ell$ enables the measurement of both F_L the longitudinal helicity fraction and the forward-backward asymmetry A_{FB}. The other helicity fractions $F_\perp$ or $F_\parallel$ can be measured from the angular distributions as well, but it has been believed that one need to perform a full angular analysis. It is, however, easy to see that a combination of F_L and $F_\perp$ can be measured if the angular distribution in terms of ϕ is studied. The angular distribution in ϕ is given by

$$\frac{d^2\Gamma}{dq^2 d\phi} = \frac{\Gamma}{2\pi}\Big[1 - \frac{1 - F_L - 2F_\perp}{2}\cos 2\phi + I_9 \sin 2\phi\Big]. \tag{18}$$

The distribution in ϕ allows us to measure $1 - F_L - 2F_\perp$. If F_L is measured independently, one can obtain $F_\perp$. The distribution also allows us to measure I_9, which is immeasurably small in SM [1] and assumed to be zero in our study. Recently, the angular analysis in ϕ has been studied [9,16] by the CDF and LHCb collaborations. In the next section we will show that $1 - F_L - 2F_\perp$ is also small in the SM as a consequence of heavy quark effective theory. We will conclude in Sec. II that the angular distribution will be almost constant for $q^2 \approx 0$, with small variation in $\cos\phi$ at large q^2.

There is yet another technique to measure $F_\perp$ which involves studying angular distributions in terms of only one angular variable. However, this approach requires independent analysis in the transversity frame defined with J/ψ at rest. In this frame the lepton makes an angle θ_{tr} with the z axis. The expression for the differential decay rate as a function of $\cos\theta_{\mathrm{tr}}$ is given by

$$\frac{d\Gamma}{dq^2 d\cos\theta_{\mathrm{tr}}} = \Gamma\Big[\frac{3}{8}(1 - F_\perp)(1 + \cos^2\theta_{\mathrm{tr}}) + \frac{3}{4}F_\perp(1 - \cos^2\theta_{\mathrm{tr}})\Big]. \tag{19}$$

Clearly, $F_\perp$ the perpendicular polarization fraction can be measured from a fit to $\cos\theta_{\mathrm{tr}}$ in the transversity frame. The errors in F_L and $F_\perp$ measured in this fashion will be correlated and the correlation will have to be taken care of.

IV. NOTATION: OBSERVABLES IN TERMS OF FORM FACTORS

The six transversity amplitudes in Eqs. (6a)–(6c) are written in terms of the Wilson coefficients and the form factors in most general form as

$$\mathcal{A}_\perp^{L,R} = C_{L,R}\mathcal{F}_\perp - \tilde{\mathcal{G}}_\perp, \tag{20a}$$
$$\mathcal{A}_\parallel^{L,R} = C_{L,R}\mathcal{F}_\parallel - \tilde{\mathcal{G}}_\parallel, \tag{20b}$$
$$\mathcal{A}_0^{L,R} = C_{L,R}\mathcal{F}_0 - \tilde{\mathcal{G}}_0 \tag{20c}$$

where to leading order, $C_{L,R} = C_9^{\mathrm{eff}} \mp C_{10}$ and $\tilde{\mathcal{G}}_\lambda = C_7^{\mathrm{eff}}\mathcal{G}_\lambda$. C_7^{eff}, C_9^{eff}, and C_{10} are the Wilson coefficients that represent short-distance corrections. $\mathcal{F}_\lambda$ and $\tilde{\mathcal{G}}_\lambda$ are defined below in terms of q^2-dependent QCD form factors that parametrize the $B \to K^*$ matrix element [3] and are suitably defined to include both factorizable and nonfactorizable contributions at any given order. The treatment of the form factors depends largely on the recoil energy of the K^* or equivalently q^2 and will have to be treated differently in the limit of heavy quark effective theory. In the large recoil limit (see Sec. IV A) the next-to-leading order effects including factorizable and nonfactorizable corrections can be parametrically included by replacements $C_9^{\mathrm{eff}} \to C_9$ and defining $\tilde{\mathcal{G}}_\lambda = C_7^{\mathrm{eff}}\mathcal{G}_\lambda + \cdots$, with the dots representing the next-to-leading and higher order terms. Hence, the Wilson coefficient and form factor can be lumped together into a single factor $\tilde{\mathcal{G}}_\lambda$. We note that even at leading order it is impossible to determine C_7^{eff} with the value of $\mathcal{G}_\lambda$ being determined. The treatment of form factors in the low-recoil limit (see Sec. IV B for details) differs significantly from the large recoil. In the low-recoil limit the leading corrections are the nonperturbative effects up to and including terms suppressed by Λ_{QCD}/Q (where $Q = \{m_b, \sqrt{q^2}\}$) and include the next-to-leading order corrections from the charm quark mass m_c and the strong coupling at $\mathcal{O}(m_c^2/Q^2, \alpha_s)$.

The form factors $\mathcal{F}_\lambda$ and $\tilde{\mathcal{G}}_\lambda$ can be related to the form factors V, $A_{1,2}$, and $T_{1,2,3}$ introduced in Eqs. (6a)–(6c) [3] by comparing these expressions for $\mathcal{A}_\lambda^{L,R}$ with those in Eqs. (20a)–(20c). Including higher order QCD correction and nonfactorizable corrections, $\mathcal{F}_\lambda$ and $\tilde{\mathcal{G}}_\lambda$ can be written as

$$\tilde{\mathcal{G}}_{\perp} = -N\sqrt{2\lambda(m_B^2, m_{K^*}^2, q^2)}\frac{2m_b}{q^2}C_7^{\text{eff}}T_1(q^2) + \cdots, \tag{21a}$$

$$\tilde{\mathcal{G}}_{\parallel} = N\sqrt{2}(m_B^2 - m_{K^*}^2)\frac{2m_b}{q^2}C_7^{\text{eff}}T_2(q^2) + \cdots, \tag{21b}$$

$$\mathcal{F}_{\perp} = N\sqrt{2\lambda(m_B^2, m_{K^*}^2, q^2)}\frac{V(q^2)}{m_B + m_{K^*}}, \tag{21c}$$

$$\mathcal{F}_{\parallel} = -N\sqrt{2}(m_B + m_{K^*})A_1(q^2), \tag{21d}$$

$$\mathcal{F}_0 = \frac{-N}{2m_{K^*}\sqrt{q^2}}\left[(m_B^2 - m_{K^*}^2 - q^2)(m_B + m_{K^*})A_1(q^2) - \lambda(m_B^2, m_{K^*}^2, q^2)\frac{A_2(q^2)}{m_B + m_{K^*}}\right], \tag{21e}$$

$$\tilde{\mathcal{G}}_0 = \frac{N}{2m_{K^*}\sqrt{q^2}}2m_b\left[(m_B^2 + 3m_{K^*}^2 - q^2)C_7^{\text{eff}}T_2(q^2) - \lambda(m_B^2, m_{K^*}^2, q^2)\frac{C_7^{\text{eff}}T_3(q^2)}{m_B^2 - m_{K^*}^2}\right] + \cdots. \tag{21f}$$

With the help of Eqs. (20a)–(20c), the observables F_L, $F_{\parallel}$, $F_{\perp}$, A_{FB}, A_4, and A_5 can be written in terms of the Wilson coefficients and from factors as

$$F_L\Gamma_f = 2(C_9^2 + C_{10}^2)\mathcal{F}_0^2 + 2\tilde{\mathcal{G}}_0^2 - 4C_9\mathcal{F}_0\tilde{\mathcal{G}}_0, \tag{22a}$$

$$F_{\parallel}\Gamma_f = 2(C_9^2 + C_{10}^2)\mathcal{F}_{\parallel}^2 + 2\tilde{\mathcal{G}}_{\parallel}^2 - 4C_9\mathcal{F}_{\parallel}\tilde{\mathcal{G}}_{\parallel}, \tag{22b}$$

$$F_{\perp}\Gamma_f = 2(C_9^2 + C_{10}^2)\mathcal{F}_{\perp}^2 + 2\tilde{\mathcal{G}}_{\perp}^2 - 4C_9\mathcal{F}_{\perp}\tilde{\mathcal{G}}_{\perp}, \tag{22c}$$

$$\frac{\pi A_4\Gamma_f}{2\sqrt{2}} = \tilde{\mathcal{G}}_{\parallel}\tilde{\mathcal{G}}_0 + (C_9^2 + C_{10}^2)\mathcal{F}_0\mathcal{F}_{\parallel} - C_9(\mathcal{F}_{\parallel}\tilde{\mathcal{G}}_0 + \tilde{\mathcal{G}}_{\parallel}\mathcal{F}_0), \tag{22d}$$

$$\frac{\sqrt{2}A_5\Gamma_f}{3} = C_{10}(\mathcal{F}_{\perp}\tilde{\mathcal{G}}_0 + \tilde{\mathcal{G}}_{\perp}\mathcal{F}_0) - 2C_9C_{10}\mathcal{F}_0\mathcal{F}_{\perp}, \tag{22e}$$

$$\frac{A_{\text{FB}}\Gamma_f}{3} = C_{10}(\mathcal{F}_{\parallel}\tilde{\mathcal{G}}_{\perp} + \mathcal{F}_{\perp}\tilde{\mathcal{G}}_{\parallel}) - 2C_9C_{10}\mathcal{F}_{\parallel}\mathcal{F}_{\perp}. \tag{22f}$$

We use Eqs. (22a)–(22f) to solve the Wilson coefficients in terms of the observables and the form factors. This solutions are achieved by defining new variables

$$r_{\parallel} = \frac{\tilde{\mathcal{G}}_{\parallel}}{\mathcal{F}_{\parallel}} - C_9, \tag{23a}$$

$$r_{\perp} = \frac{\tilde{\mathcal{G}}_{\perp}}{\mathcal{F}_{\perp}} - C_9, \tag{23b}$$

$$r_0 = \frac{\tilde{\mathcal{G}}_0}{\mathcal{F}_0} - C_9, \tag{23c}$$

$$r_{\wedge} = \frac{\tilde{\mathcal{G}}_{\parallel} + \tilde{\mathcal{G}}_0}{\mathcal{F}_{\parallel} + \mathcal{F}_0} - C_9. \tag{23d}$$

In terms of these new variables $r_{\parallel}$, $r_{\perp}$, r_0, and $r_{\wedge}$ the observables in Eqs. (22a)–(22f) can be written conveniently as

$$F_{\parallel}\Gamma_f = 2\mathcal{F}_{\parallel}^2(r_{\parallel}^2 + C_{10}^2), \tag{24a}$$

$$F_{\perp}\Gamma_f = 2\mathcal{F}_{\perp}^2(r_{\perp}^2 + C_{10}^2), \tag{24b}$$

$$F_L\Gamma_f = 2\mathcal{F}_0^2(r_0^2 + C_{10}^2), \tag{24c}$$

$$(F_L + F_{\parallel} + \sqrt{2}\pi A_4)\Gamma_f = 2(\mathcal{F}_0 + \mathcal{F}_{\parallel})^2(r_{\wedge}^2 + C_{10}^2), \tag{24d}$$

$$\sqrt{2}A_5\Gamma_f = 3\mathcal{F}_{\perp}\mathcal{F}_0C_{10}(r_0 + r_{\perp}), \tag{24e}$$

$$A_{\text{FB}}\Gamma_f = 3\mathcal{F}_{\perp}\mathcal{F}_{\parallel}C_{10}(r_{\parallel} + r_{\perp}), \tag{24f}$$

$$(A_{\text{FB}} + \sqrt{2}A_5)\Gamma_f = 3\mathcal{F}_{\perp}(\mathcal{F}_0 + \mathcal{F}_{\parallel})C_{10}(r_{\wedge} + r_{\perp}). \tag{24g}$$

It is easy to see that only six of the seven equations above are independent; the last Eq. (24g) is easily obtained from Eqs. (24e) and (24f). Considerable notational simplification is achieved by defining the following six ratios of form factors:

$$\mathsf{P}_1 = \frac{\mathcal{F}_{\perp}}{\mathcal{F}_{\parallel}}, \qquad \mathsf{P}_2 = \frac{\mathcal{F}_{\perp}}{\mathcal{F}_0}, \qquad \mathsf{P}_3 = \frac{\mathcal{F}_{\perp}}{\mathcal{F}_0 + \mathcal{F}_{\parallel}} = \frac{\mathsf{P}_1\mathsf{P}_2}{\mathsf{P}_1 + \mathsf{P}_2} \tag{25}$$

$$\mathsf{P}_1' = \frac{\tilde{\mathcal{G}}_{\perp}}{\tilde{\mathcal{G}}_{\parallel}}, \qquad \mathsf{P}_2' = \frac{\tilde{\mathcal{G}}_{\perp}}{\tilde{\mathcal{G}}_0}, \qquad \mathsf{P}_3' = \frac{\tilde{\mathcal{G}}_{\perp}}{\tilde{\mathcal{G}}_{\parallel} + \tilde{\mathcal{G}}_0} = \frac{\mathsf{P}_1'\mathsf{P}_2'}{\mathsf{P}_1' + \mathsf{P}_2'}. \tag{26}$$

Clearly, $r_{\wedge}$ introduced in Eq. (23) is not independent and is easily obtained from a combination of $r_{\parallel}$ and r_0. The expression for $r_{\wedge}$ in terms of $r_{\parallel}$ and r_0 and form factors ratios P_1 and P_2 is easily derived to be

$$r_{\wedge} = \frac{r_{\parallel}\mathsf{P}_2 + r_0\mathsf{P}_1}{\mathsf{P}_2 + \mathsf{P}_1}. \tag{27}$$

Naively, we have nine theoretical parameters, the three Wilson coefficients C_7, C_9, and C_{10} and the six form factors $\mathcal{F}_0$, $\mathcal{F}_{\parallel}$, $\mathcal{F}_{\perp}$, $\mathcal{G}_0$, $\mathcal{G}_{\parallel}$, and $\mathcal{G}_{\perp}$, describing the six observables Γ_f, F_L, $F_{\perp}$, A_4, A_5, and A_{FB}. As mentioned earlier, C_7^{eff} and $\mathcal{G}_{\lambda}$ cannot be distinguished and they are lumped together beyond leading order, so that we have only eight independent theoretical parameters, the two Wilson coefficients C_9 and C_{10} and six form factors $\mathcal{F}_0$, $\mathcal{F}_{\parallel}$, $\mathcal{F}_{\perp}$, $\tilde{\mathcal{G}}_0$, $\tilde{\mathcal{G}}_{\parallel}$, and $\tilde{\mathcal{G}}_{\perp}$. It is obvious that with two theoretical inputs in addition to the observables we should, in principle, be able to solve for the remaining six theoretical parameters purely in terms of these two reliable inputs and observables. Fortunately, advances in our understanding of these form factors permit us a judicious choice of the two reliable inputs which depends on the energy of recoiling K^* (or equivalent q^2). At large recoil the two inputs are the ratios of form factors P_1 and P_1'

which are well predicted at next-to-leading order in QCD corrections and free from form factors $\xi_\parallel$ and $\xi_\perp$ in heavy quark effective theory. While the choice of P_1 and P_1' works well at low q^2, at low recoil another condition equating the three ratios $\tilde{\mathcal{G}}_\lambda/\mathcal{F}_\lambda$ for $\lambda = \{0, \parallel, \perp\}$ is needed.

The decay mode $B \to K^*\ell^+\ell^-$ has been studied with form factors calculated in different models. For example, in Ref. [17] the mode has been studied using light-cone hadron distribution amplitudes [18] combined with QCD sum rules on the light cone [19]. In Ref. [20] the mode was studied using naive factorization and QCD sum rules on the light cone. In Refs. [15,21,22] it has been studied in the heavy quark limit using QCD factorization [23,24]. Soft-collinear effective theory [25–29] that is valid for small q^2 (large recoil of K^*) has been used to study the decay in Ref. [30], while operator product expansion that is valid for large q^2 (low recoil) has been studied in Ref. [31].

In the next two subsections that follow, we will digress to consider the $B \to K^*\ell^+\ell^-$ form factors and their relations in the two limits of the K^* meson recoil energy. We will present our model independent analysis in the next section (Sec. V). We will assume P_1 and P_1' as inputs for most of the paper as the results are valid throughout the q^2 domain, except when $\mathsf{P}_1 = \mathsf{P}_1'$. We will show that the validity of the large recoil limit approximation can be verified by a direct measurement of P_1 in terms of helicity fractions, at the zero-crossing point of $A_{\rm FB}$, i.e., at $A_{\rm FB} = 0$. The low-recoil limit is considered at the end in Sec. VI, where we will also examine the special case $\mathsf{P}_1 = \mathsf{P}_1'$. The validity of the low-recoil limit can also be tested through a relation derived purely between observables which is valid only in the low-recoil limit. In both the recoil regions we derive several important relations between observables, Wilson coefficients, and form factors. We find that the six observables are not independent as there exists one constraint relation that involves observables alone and, hence, free from the details of recoil energy approximation as well. As a consequence, we find that $\mathcal{F}_\parallel$ cannot be solved for and must be taken as an additional input as well.

A. Form factor in the large recoil limit

In $B \to K^*$ transition at low q^2, the light meson K^* carries a large energy E_{K^*}. Since the initial B meson contains the heavy b quark, in this limit the form factors can be expanded in small ratios of $\Lambda_{\rm QCD}/m_b$ and $\Lambda_{\rm QCD}/E_{K^*}$ [32]. This reduces the independent $B \to K^*$ form factors from seven to two universal form factors $\xi_\perp$ and $\xi_\parallel$. In terms of these two form factors, the seven form factors can be written up to $1/m_b$ and α_s corrections as [32,33]

$$A_1(q^2) = \frac{2E_{K^*}}{m_B + m_{K^*}}\xi_\perp(E_{K^*}), \tag{28a}$$

$$A_2(q^2) = \frac{m_B}{m_B - m_{K^*}}[\xi_\perp(E_{K^*}) - \xi_\parallel(E_{K^*})], \tag{28b}$$

$$A_0(q^2) = \frac{E_{K^*}}{m_{K^*}}\xi_\parallel(E_{K^*}), \tag{28c}$$

$$V(q^2) = \frac{m_B + m_{K^*}}{m_B}\xi_\perp(E_{K^*}), \tag{28d}$$

$$T_1(q^2) = \xi_\perp(E_{K^*}), \tag{28e}$$

$$T_2(q^2) = \frac{2E_{K^*}}{m_B}\xi_\perp(E_{K^*}), \tag{28f}$$

$$T_3(q^2) = \xi_\perp(E_{K^*}) - \xi_\parallel(E_{K^*}), \tag{28g}$$

where, E_{K^*} is the energy of the K^* meson,

$$E_{K^*} = \frac{m_B^2 + m_{K^*}^2 - q^2}{2m_B}.$$

We note that the form factor A_0 does not appear in our expressions in the massless lepton limit. In the large recoil limit T_2/T_1 and V/A_1 are well predicted and reduce to the simple form

$$\frac{T_2}{T_1} = \frac{2E_{K^*}}{m_B}, \tag{29}$$

$$\frac{V}{A_1} = \frac{(m_B + m_{K^*})^2}{2E_{K^*}m_B}. \tag{30}$$

Note that these ratios are independent of the universal form factors $\xi_\parallel$ and $\xi_\perp$ and are valid to all orders in the strong coupling constant [15].

In addition to the order α_s corrections to the hadronic form factors, there also exist "nonfactorizable" corrections, which can be significant in the heavy quark and large recoil limit. Following Ref. [15], these nonfactorizable corrections can be incorporated in next-to-leading order in QCD by the following transformations [34]:

$$C_7^{\rm eff}T_i \to \mathcal{T}_i, \tag{31a}$$

$$C_9^{\rm eff} \to C_9, \tag{31b}$$

where the Wilson coefficients are taken at the next-to-next-to leading order, and the $\mathcal{T}_i$ are defined as

$$\mathcal{T}_1 = \mathcal{T}_\perp, \qquad \mathcal{T}_2 = \frac{2E_{K^*}}{m_B}\mathcal{T}_\perp, \qquad \mathcal{T}_3 = \mathcal{T}_\perp + \mathcal{T}_\parallel. \tag{32}$$

The complete expressions of $\mathcal{T}_{\perp,\parallel}$ are given in Ref. [15].

The form factor ratios $\mathsf{P}_{1,2,3}$ and $\mathsf{P}'_{1,2,3}$ can be written with the help of the Eqs. (28a)–(28g). The expressions for the ratio's P_1 and P_1' are of particular interest, since these form factor ratios do not receive any QCD corrections in the heavy quark effective theory and are independent of both of the form factors $\xi_\parallel$ and $\xi_\perp$ to all orders in α_s and to leading order in the $1/m_b$ expansion. We will take expressions for P_1 and P_1' as input and find that they are given by the simple form

$$\mathsf{P}_1 = \frac{\mathcal{F}_\perp}{\mathcal{F}_\parallel} = \frac{\sqrt{\lambda(m_B^2, m_{K^*}^2, q^2)}}{(m_B + m_{K^*})^2}\frac{V(q^2)}{A_1(q^2)} \equiv \left[\frac{-\sqrt{\lambda(m_B^2, m_{K^*}^2, q^2)}}{2E_{K^*}m_B}\right], \tag{33a}$$

$$\mathsf{P}_1' = \frac{\tilde{\mathcal{G}}_\perp}{\tilde{\mathcal{G}}_\parallel} = \frac{-\sqrt{\lambda(m_B^2, m_{K^*}^2, q^2)}}{m_B^2 - m_{K^*}^2}\frac{\mathcal{T}_1}{\mathcal{T}_2} = \left[\frac{-\sqrt{\lambda(m_B^2, m_{K^*}^2, q^2)}m_B}{2E_{K^*}(m_B^2 - m_{K^*}^2)}\right]. \tag{33b}$$

It may be noted that the form factor ratios P_1 and P_1' do not depend on the universal form factors $\xi_\parallel$ and $\xi_\perp$ and are unaltered by the inclusion of nonfactorizable corrections and higher order corrections in QCD. P_1 and P_1' are hence used by us as reliable theoretical inputs. On the other hand, it is easy to see that $\mathsf{P}_{2,3}$ and $\mathsf{P}_{2,3}'$ depend on universal form factors and hence receive corrections from higher order and nonfactorizable contributions that result in a more complicated expression. In our approach $\mathsf{P}_{2,3}$ and $\mathsf{P}_{2,3}'$ will be obtained in terms of observables and P_1 and P_1' in Eqs. (87), (88), (90), and (91).

The expressions (33a) and (33b) are valid for large recoil region where q^2 is small and are usually considered extremely accurate for q^2 between 1 GeV and 6 GeV [33]. The region $q^2 < 1$ GeV is ignored to eliminate resonance contributions which might not only introduce uncertainties but might also introduce complex contributions which we have assumed are absent. Unless otherwise stated, large recoil region would mean $0.10\ \mathrm{GeV}^2 \le q^2 \le 12.86\ \mathrm{GeV}^2$. We stress that once the nonfactorizable corrections are taken into account, the Wilson coefficient C_7 can no longer be separated from the hadronic form factor. The C_7 and the the hadronic form factors lump together into effective photon vertex $\tilde{\mathcal{G}}_\lambda$, which as we will show, can be expressed in terms of observables and the form factors P_1 and P_1'.

B. Form factor in the low-recoil limit

A model independent description for the case of low-recoil energy of the K^* in $B \to K^*\ell^+\ell^-$ decay was put forward by Grinstein and Pirjol [31] in the modified heavy quark effective theory framework. In this approach [31], "near the zero point $q^2 \approx (m_B - m_{K^*})^2$, the long-distance contributions to $B \to K^*\ell^+\ell^-$ can be computed as short-distance effect using simultaneous heavy quark and operator product expansion in $1/Q$ with $Q = \{m_b, \sqrt{q^2}\}$." In view of this the subleading m_{K^*}/m_B terms are neglected and nonfactorizable corrections are ignored. An elaborate study of the predictions for $B \to K^*\ell^+\ell^-$ was undertaken in Ref. [35] where the next-to-leading order corrections from the charm quark mass m_c and strong coupling at $\mathcal{O}(m_c/Q^2, \alpha_s)$ were included. The result is a relation between the $B \to K^*\ell^+\ell^-$ form factors that reduces the number of independent hadronic form factors to only three, i.e., V, A_1, and A_2 can be expressed in terms of the form factors T_1, T_2, T_3 as

$$T_1(q^2) = \kappa V(q^2), \tag{34a}$$

$$T_2(q^2) = \kappa A_1(q^2), \tag{34b}$$

$$T_3(q^2) = \kappa A_2(q^2)\frac{m_B^2}{q^2} \tag{34c}$$

where the expression of κ is given in [35].

In the low-recoil limit the nonfactorizable corrections and higher order corrections in α_s are ignorable, hence, we have $\tilde{\mathcal{G}}_\lambda = C_7^{\mathrm{eff}}\mathcal{G}_\lambda$ for all $\lambda = \{0, \parallel, \perp\}$. The condition in Eq. (34) together with Eq. (21) on ignoring m_{K^*}/m_B terms can be recast as

$$\frac{\mathcal{G}_\parallel}{\mathcal{F}_\parallel} = \frac{\mathcal{G}_\perp}{\mathcal{F}_\perp} = \frac{\mathcal{G}_0}{\mathcal{F}_0} \equiv \hat{\kappa} = -\kappa\frac{2m_B m_b}{q^2}. \tag{35}$$

This can easily be seen to imply that

$$\mathsf{P}_1 = \mathsf{P}_1', \qquad \mathsf{P}_2 = \mathsf{P}_2', \qquad \mathsf{P}_3 = \mathsf{P}_3', \tag{36}$$

and hence,

$$r_\parallel = r_\perp = r_0 = r_\wedge \equiv r. \tag{37}$$

In the low-recoil limit the form factor ratios P_1 and P_1' are easily derived to be

$$\mathsf{P}_1 = \mathsf{P}_1' = \frac{-\sqrt{\lambda(m_B^2, m_{K^*}^2, q^2)}}{(m_B + m_{K^*})^2}\frac{V(q^2)}{A_1(q^2)}. \tag{38}$$

Note that in this limit as well, the two ratios P_1 and P_1' are independent of the universal form factors $\xi_\parallel$ and $\xi_\perp$. The low-recoil approximation is expected to work well in region $14.18\ \mathrm{GeV}^2 \le q^2 \le 19\ \mathrm{GeV}^2$. Conventionally, the low-recoil region is meant to imply this range of q^2. In Sec. VI we will reconsider the low-recoil region to study the special feature that emerge in the low-recoil region. In the low-recoil limit we need to take special care of the fact that $\mathsf{P}_1 = \mathsf{P}_1'$.

V. MODEL INDEPENDENT ANALYSIS

In this section we present a new model independent approach that offers a possibility of isolating hadronic effects from genuine new physics contributions. We begin by deriving the solutions for the Wilson coefficients C_9, C_{10} and the effective photon vertex $\tilde{\mathcal{G}}_\parallel$, in terms of observables and the minimum number of required form factor ratios, some of which are more or less independent of hadronic uncertainties.

The first set of solutions are obtained using three independent Eqs. (24a), (24b), and (24f), and one easily solves (see Appendix A) for $r_\| + r_\perp$ to be

$$r_\| + r_\perp = \pm \frac{\sqrt{\Gamma_f}}{\sqrt{2}\mathcal{F}_\perp}\bigg(\mathsf{P}_1^2 F_\| + F_\perp \pm \mathsf{P}_1\sqrt{4F_\| F_\perp - \frac{16}{9}A_{\rm FB}^2}\bigg)^{1/2}.$$

However, $r_\| + r_\perp = 0$ when $A_{\rm FB} = 0$ from Eq. (24f). The term inside the round bracket of the above equation becomes a whole square if $A_{\rm FB} = 0$, hence,

$$r_\| + r_\perp|_{A_{\rm FB}=0} = \pm \frac{\sqrt{\Gamma_f}}{\sqrt{2}\mathcal{F}_\perp}(\sqrt{F_\perp} \pm \mathsf{P}_1\sqrt{F_\|}) = 0. \quad (39)$$

Since, the expression for $r_\| + r_\perp$ should be valid for all values of the observables, the right-hand side could go to zero only if positive sign ambiguity is chosen, taking into account that P_1 is negative. This fixes the sign ambiguity inside the round bracket. The condition $r_\| + r_\perp = 0$ gives us the familiar relation for the zero crossing of $A_{\rm FB}$. The definitions of $r_\|$ and $r_\perp$ straightforwardly imply that $A_{\rm FB} = 0$ at

$$\begin{aligned} 2C_9 &= C_7\bigg(\frac{\mathcal{G}_\perp}{\mathcal{F}_\perp} + \frac{\mathcal{G}_\|}{\mathcal{F}_\|}\bigg), \\ &= -\frac{4m_b}{q^2}C_7\frac{T_1(q^2)}{V(q^2)}(m_B + m_{K^*})\bigg(1 - \frac{m_{K^*}^2}{2m_B^2}\bigg), \\ &= -\frac{4m_b m_B}{q^2}C_7\bigg(1 - \frac{m_{K^*}^2}{2m_B^2}\bigg) + \mathcal{O}(\alpha_s), \end{aligned} \quad (40)$$

where we have used Eqs. (29) and (30). The $\mathcal{O}(\alpha_s)$ dependence arises from the ratio $T_1(q^2)/V(q^2)$, which also depends on $\xi_\perp(q^2)$ [33].

Notice that, Eq. (39) implies that when $A_{\rm FB} = 0$, we must have a exact equality

$$\mathsf{P}_1 = -\frac{\sqrt{F_\perp}}{\sqrt{F_\|}}\bigg|_{A_{\rm FB}=0} \quad (41)$$

enabling a measurement of P_1 in terms of the ratio of helicity fractions. If zero crossing were to occur, it would provide an interesting test of our understanding of form factors. Very recently, LHCb has confirmed [16] zero crossing of $A_{\rm FB}$ for the first time. The zero crossing is observed at $q^2 = 4.9^{+1.1}_{-1.3}$ GeV^2, which is consistent with the predictions of the standard model and lies in the large recoil region. Equation (41) can, hence, be used to measure P_1 at the zero crossing of $A_{\rm FB}$. A confirmation of the estimate of P_1 with direct helicity measurements would leave no doubt on the reliable predictability HQET in the large recoil region.

The solution of C_{10} in terms of the observables and hadronic form factors now reads as

$$C_{10} = \frac{\sqrt{\Gamma_f}}{\sqrt{2}\mathcal{F}_\|}\frac{2}{3}\frac{A_{\rm FB}}{[\pm\sqrt{\mathsf{P}_1^2 F_\| + F_\perp + \mathsf{P}_1 Z_1}]}, \quad (42)$$

where Z_1 is defined as

$$Z_1 = \sqrt{4F_\| F_\perp - \frac{16}{9}A_{\rm FB}^2}. \quad (43)$$

This solution allows us to measure C_{10} directly in terms of observables, "clean" form factors P_1, P_1' and on $\mathcal{F}_\|$. In Tables I and II we have present the predicted values of $F_\perp$ and C_{10} using F_L and $A_{\rm FB}$ values from [10,16], respectively. In Table II we also estimate $F_\perp$ which is computed directly from data using Eq. (18) and the value of S_3 quoted in Ref. [16].

A rather unexpected observation is that as long as $4F_\| F_\perp \geq \frac{16}{9}A_{\rm FB}^2$, the term $\mathsf{P}_1^2 F_\| + F_\perp + \mathsf{P}_1 Z_1$ is always positive. This is easily seen by an (infinite) series expansion in $A_{\rm FB}$:

$$\begin{aligned} \mathsf{P}_1^2 F_\| + F_\perp + \mathsf{P}_1 Z_1 &= (\mathsf{P}_1\sqrt{F_\|} + \sqrt{F_\perp})^2 - \frac{4A_{\rm FB}^2\mathsf{P}_1}{9\sqrt{F_\| F_\perp}} \\ &\quad - \frac{4A_{\rm FB}^4\mathsf{P}_1}{81(F_\| F_\perp)^{3/2}} + \mathcal{O}(A_{\rm FB}^6) \geq 0, \end{aligned} \quad (44)$$

where every term is positive since P_1 is negative. Since the Wilson coefficient C_{10} is real in the standard model, Z_1 must be real restricting the observables $F_\|$, $F_\perp$, and $A_{\rm FB}$ such that

TABLE I. The predictions for $F_\perp$ [Eq. (52)] and C_{10} [Eq. (42)] using 0.37 fb^{-1} LHCb [10] data for F_L, $A_{\rm FB}$, and $d\Gamma/dq^2$. "(T)" in the first column indicates the values quoted are theoretical estimates. The form factor $\mathcal{F}_\|$ and the ratios P_1 and P_1' are averaged over each q^2 bin using heavy-to-light form factors at large recoil (for 0.10 GeV$^2 \leq q^2 \leq$ 12.86 GeV^2) and heavy-to-light form factors at low recoil (for 16 GeV$^2 \leq q^2 \leq$ 19 GeV^2). The region 14.18 GeV$^2 \leq q^2 \leq$ 16 GeV^2 is neglected as the form factors cannot be calculated reliably in this region. The unusual large value of C_{10} in the 0.10 GeV$^2 \leq q^2 \leq$ 2 GeV^2 region could be due to failure in estimating $\mathcal{F}_\|$ or perhaps be a signal new physics. It is unlikely [36,37] that such a large effect can be due to the contributions from low lying resonances in the experimental data. It may be noted that the estimate of $F_\perp$ does not depend on universal form factors and is clean in the low-recoil limit.

q^2 (GeV^2)	0.10–2.00	2.00–4.30	4.30–8.68	10.09–12.86	14.18–16.00	16.00–19.00	1–6
$F_\perp$ (T)	0.44 ± 0.01	0.14 ± 0.06	0.19 ± 0.03	0.25 ± 0.04	$\cdots$	0.14 ± 0.016	0.21 ± 0.05
C_{10} (T)	14.36 ± 1.68	2.81 ± 0.78	3.00 ± 0.384	2.34 ± 0.372	$\cdots$	3.11 ± 0.39	3.81 ± 0.58

TABLE II. The same as Table I but with 1.0 fb^{-1} LHCb data [16]. "(E)" in the first column indicates the values quoted are experimental estimates. $F_\perp$ (E) is computed directly from data using Eq. (18) and the value of S_3 quoted in Ref. [16]. The values of C_{10} seem to decrease with the larger data set used and are marginally lower than theoretical estimates. Unfortunately, the cause of discrepancy in C_{10} cannot be fixed; it could either be due to failure in estimating $\mathcal{F}_\parallel$ or perhaps be a signal of new physics. Note that in the $0.10\ \mathrm{GeV}^2 \le q^2 \le 2\ \mathrm{GeV}^2$ region C_{10} is still large even with improved statistics. We emphasize that the two values of $F_\perp$ are in good agreement almost throughout the q^2 region.

q^2 (GeV^2)	0.10–2.00	2.00–4.30	4.30–8.68	10.09—12.86	14.18–16.00	16.00–19.00	1–6
$F_\perp$ (E)	$0.36^{+0.14}_{-0.11}$	$0.11^{+0.09}_{-0.15}$	0.31 ± 0.09	$0.145^{+0.12}_{-0.13}$	0.35 ± 0.13	$0.08^{+0.13}_{-0.14}$	$0.22^{+0.10}_{-0.11}$
$F_\perp$ (T)	0.31 ± 0.03	0.15 ± 0.04	0.20 ± 0.03	0.22 ± 0.03	...	0.12 ± 0.01	0.17 ± 0.03
C_{10} (T)	12.91 ± 1.07	2.60 ± 0.779	2.88 ± 0.32	2.0 ± 0.25	...	2.55 ± 0.29	3.26 ± 0.45

$$4F_\parallel F_\perp \ge \frac{16}{9}A_{\mathrm{FB}}^2. \tag{45}$$

The violation of this condition will be a clear signal of new physics. On the other hand, if the experiments find a real value that does not agree with the estimates of standard model value, it could either be a signal of new physics or of the uncertainties in form factor estimations. The Wilson coefficient C_9, can also be solved (see Appendix A) in terms of observables and form factor ratios,

$$C_9 = \frac{\sqrt{\Gamma_f}}{\sqrt{2}\mathcal{F}_\parallel}\frac{(F_\parallel \mathsf{P}_1\mathsf{P}_1' - F_\perp) - \frac{1}{2}(\mathsf{P}_1 - \mathsf{P}_1')Z_1}{[\pm(\mathsf{P}_1 - \mathsf{P}_1')\sqrt{\mathsf{P}_1^2 F_\parallel + F_\perp + \mathsf{P}_1 Z_1}]}. \tag{46}$$

All the discussions following Eq. (42) equally are applicable to this solutions. The way the matrix element decomposition is defined in the heavy quark and large energy limit, at next-to-leading logarithmic order [15], does not allow us to factor out the Wilson coefficient C_7^{eff} from the hadronic form factors T_i. Hence, the solution of C_7 is not possible. However, we can solve for the effective photon vertex $\tilde{\mathcal{G}}_\parallel$, which we can express in terms of the observables and P_1, P_1'. The solution of $\tilde{\mathcal{G}}_\parallel$ is

$$\tilde{\mathcal{G}}_\parallel = \frac{\sqrt{\Gamma_f}}{\sqrt{2}}\frac{(\mathsf{P}_1^2 F_\parallel - F_\perp)}{[\pm(\mathsf{P}_1 - \mathsf{P}_1')\sqrt{\mathsf{P}_1^2 F_\parallel + F_\perp + \mathsf{P}_1 Z_1}]}. \tag{47}$$

To obtain the three expressions, Eqs. (42), (46), and (47), we removed the sign ambiguities in the solution by looking at the behavior of the solutions at the A_{FB} zero crossing points. All of our solutions for the Wilson coefficients depend explicitly on the assumption that $A_{\mathrm{FB}} \neq 0$, hence, the Wilson coefficients can be determined at any q^2 except at the zero crossing of A_{FB}. The denominator of $\tilde{\mathcal{G}}_\parallel$ and C_9 depend on $\mathsf{P}_1 - \mathsf{P}_1'$, so the behavior of the Wilson coefficients at the point $\mathsf{P}_1 \to \mathsf{P}_1'$ needs careful examination. Unlike the zeros of A_{FB}, which can be experimentally determined and hence avoided, the crossing point for P_1 and P_1' *a priori* can only be determined based on calculations and hence, may be uncertain. We note that in this limit we have $r_\parallel - r_\perp = 0$, where as in the limit $A_{\mathrm{FB}} = 0$, we had $r_\parallel + r_\perp = 0$. Naively, C_9 and $\tilde{\mathcal{G}}_\parallel$ appear to be divergent in the limit $\mathsf{P}_1 \to \mathsf{P}_1'$, as can be seen from Eqs. (46) and (47) and indeed Eq. (A8) cannot be used to determine the Wilson coefficients C_7 and C_9. However, it is easily seen that the Wilson coefficients are finite when $\mathsf{P}_1 \to \mathsf{P}_1'$. Consider the combination $\tilde{\mathcal{G}}_\parallel - \mathcal{F}_\parallel C_9$, which is seen from Eqs. (47) and (46) to be manifestly finite in the limit $\mathsf{P}_1' \to \mathsf{P}_1$:

$$\tilde{\mathcal{G}}_\parallel - \mathcal{F}_\parallel C_9 = \sqrt{\frac{\Gamma_f}{2}}\frac{F_\parallel \mathsf{P}_1 + \frac{1}{2}Z_1}{\sqrt{\mathsf{P}_1^2 F_\parallel + F_\perp + \mathsf{P}_1 Z_1}}. \tag{48}$$

We will show that the combination $\tilde{\mathcal{G}}_\parallel - \mathcal{F}_\parallel C_9$ can be determined and indeed if $\mathcal{F}_\parallel$ is assumed $\tilde{\mathcal{G}}_\parallel$ and C_9 can be individually determined and are finite.

In the limit $\mathsf{P}_1' = \mathsf{P}_1$, Eq. (23) implies

$$r_\parallel^2 + C_{10}^2 = r_\perp^2 + C_{10}^2 = \frac{F_\parallel \Gamma_f}{2\mathcal{F}_\parallel^2} = \frac{F_\perp \Gamma_f}{2\mathcal{F}_\perp^2}. \tag{49}$$

We thus have

$$\mathsf{P}_1^2 = \mathsf{P}_1'^2 = \frac{F_\perp}{F_\parallel} = \frac{\mathcal{F}_\perp^2}{\mathcal{F}_\parallel^2}, \tag{50}$$

which enables a measurement of P_1. Indeed if the hadronic estimate $\mathsf{P}_1^2 = F_\perp/F_\parallel$ is verified by measurement even when $A_{\mathrm{FB}} \neq 0$, we can conclude with certainty that $\mathsf{P}_1 = \mathsf{P}_1'$. Hadronic estimates can thus be verified experimentally. Note that a similar condition at $A_{\mathrm{FB}} = 0$ also provided a measurement of P_1 in Eq. (41).

Many more important results can be derived from the expressions derived so far. We can use Eqs. (42) and (46) to obtain the ratio C_9/C_{10}:

$$R \equiv \frac{C_9}{C_{10}} = \frac{2(F_\parallel \mathsf{P}_1\mathsf{P}_1' - F_\perp) - (\mathsf{P}_1 - \mathsf{P}_1')Z_1}{\frac{4}{3}A_{FB}(\mathsf{P}_1 - \mathsf{P}_1')}. \tag{51}$$

We emphasize that C_9/C_{10}, defined henceforth as R, is expressed as a "clean parameter" in terms of observables and the two ratios of form factors which are predicted exactly in heavy quark effective theory. Our expressions so far depend on the helicity fractions $F_\parallel$ and $F_\perp$; however,

F_L has been measured and since $F_L + F_\parallel + F_\perp = 1$, we can express $F_\parallel$ in terms of F_L and $F_\perp$. All of our conclusions throughout the paper can be reexpressed in terms of just two helicity fractions F_L and $F_\perp$. Equation (51) can be used to experimentally test the ratio of C_9 and C_{10}. On the other hand, if the ratio $R = C_9/C_{10}$ is known very accurately, $F_\perp$ can be predicted using Eq. (51) in terms of F_L and $A_{\rm FB}$ as

$$F_\perp = \frac{-4RA_{\rm FB}(\mathsf{P}_1 - \mathsf{P}_1')(1 + \mathsf{P}_1\mathsf{P}_1') + 3(1 - F_L)(\mathsf{P}_1 + \mathsf{P}_1')^2 - (\mathsf{P}_1 - \mathsf{P}_1')\sqrt{T_\perp}}{3(1 + \mathsf{P}_1^2)(1 + \mathsf{P}_1'^2)}, \tag{52}$$

where

$$T_\perp = 9(1 - F_L)^2(\mathsf{P}_1' + \mathsf{P}_1)^2 - 24RA_{\rm FB}(1 - F_L)(\mathsf{P}_1 - \mathsf{P}_1')(1 - \mathsf{P}_1\mathsf{P}_1') - 16A_{\rm FB}^2[R^2(\mathsf{P}_1 - \mathsf{P}_1')^2 + (1 + \mathsf{P}_1^2)(1 + \mathsf{P}_1'^2)].$$

The sign of the term containing $\sqrt{T_\perp}$ could either be positive or negative. Of the two possible solutions for $F_\perp$, in Eq. (52) we have chosen the solution which gives the correct value of R obtained from Eq. (51). This solution corresponds to the one with the negative ambiguity as shown in Eq. (52). As seen from Eq. (52), the transversity amplitude $F_\perp$ is expressed in terms of two observables F_L and $A_{\rm FB}$ which has already been measured. Using the measured values of F_L and $A_{\rm FB}$ from Refs. [10,16], we have tabulated the predicted values of $F_\perp$ in Tables I and II, respectively.

In order that $F_\perp$ take real values, $T_\perp$ must be positive. The positivity of $T_\perp$ imposes constraints on the possible values for F_L and $A_{\rm FB}$, which cannot, therefore, be arbitrarily chosen. The requirement for a real solution for $F_\perp$, hence, implies a constraint on $A_{\rm FB}$ in terms of P_1, P_1', R, and observable F_L:

$$\frac{-3(1 - F_L)}{4}T_- \le A_{FB} \le \frac{3(1 - F_L)}{4}T_+,$$
$$T_\pm = \frac{(\mathsf{P}_1 + \mathsf{P}_1')^2}{\sqrt{(1 + \mathsf{P}_1^2)(1 + \mathsf{P}_1'^2)}\sqrt{(\mathsf{P}_1 + \mathsf{P}_1')^2 + R^2(\mathsf{P}_1 - \mathsf{P}_1')^2} \mp (1 - \mathsf{P}_1\mathsf{P}_1')(\mathsf{P}_1 - \mathsf{P}_1')R}. \tag{53}$$

It is easy to see that $T_\pm \approx 1$ when $\mathsf{P}_1 \approx \mathsf{P}_1' \approx -1$. Given the values of P_1 and P_1' from Table III, we expect $T_\pm \approx 1$. The allowed domain for $A_{\rm FB}$ is hence almost free from R as long as $\mathsf{P}_1 \approx \mathsf{P}_1' \approx -1$. In Fig. 1, we have depicted the permitted $F_L - A_{\rm FB}$ parameter space by the solid (blue) triangle for $R = -1$. In the figure to the left P_1 and P_1' values are averaged over 1 to 6 GeV^2 using heavy-to-light form factors at large recoil (see Sec. IV A), and in the figure to the right we have used P_1 and P_1' values averaged over 16 to 19 GeV^2 using heavy-to-light form factors at low recoil (see Sec. IV B). Inside the triangles, the solid (black) lines correspond to the $F_\perp$ values; the dashed (blue) lines correspond to the C_{10} values as function of F_L and $A_{\rm FB}$. In Fig. 2 the variation of the parameter space is studied as a function of R. The large-dashed (red) triangle and the identical lines correspond to $R = 10$. The $R = -10$ case is depicted by the small dashed (blue) line. The $R = -1$ case is shown for reference with solid (black) lines. In the figure to the left P_1 and P_1' values are averaged over 1 to 6 GeV^2 and in the figure to the right we have used P_1 and P_1' values averaged over 16 to 19 GeV^2.

TABLE III. The form factor ratios P_1, P_1' and $\mathcal{F}_\parallel$ averaged over different q^2 bins at large recoil.

GeV^2	0.10–2	2–4.3	4.3–8.68	10.09–12.86	1–6
P_1	−0.8924	−0.9286	−0.9034	−0.8337	−0.9259
P_1'	−0.9189	−0.9561	−0.9302	−0.8585	−0.9533
$\mathcal{F}_\parallel(10^{-12})$	−5.7667	−11.330	−17.4311	−25.8917	−11.8692

Interestingly, Eq. (51) can also be inverted to express A_{FB} in terms of P_1, P_1', and R:

$$A_{\rm FB} = \frac{3(RX - \sqrt{Y(\mathsf{P}_1 - \mathsf{P}_1')^2(1 + R^2) - X^2})}{4(\mathsf{P}_1 - \mathsf{P}_1')(1 + R^2)}. \tag{54}$$

where $X = 2(F_\parallel\mathsf{P}_1\mathsf{P}_1' - F_\perp)$ and $Y = 4F_\parallel F_\perp$. Note that the Eq. (51) is quadratic in $A_{\rm FB}$, and should have resulted in a two-fold ambiguity in the solution. One easily confirms that only the solution with a positive sign in front of the square root is valid by substituting the observables in terms of the form factors and the Wilson coefficients. The usefulness of the result in Eq. (54) is that it constrains the $F_L - F_\perp$ parameter space. This is easily derived by requiring that $A_{\rm FB}$ in Eq. (54) is real, implying the positivity of the argument of the radical in the expression for $A_{\rm FB}$:

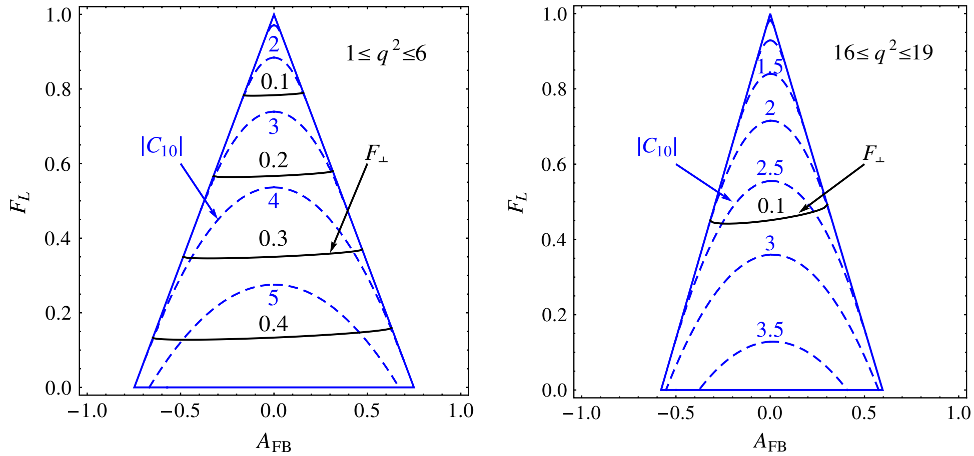

FIG. 1 (color online). The allowed $F_L - A_{FB}$ parameter space depicted by the solid (blue) triangle for $R = -1$ is obtained by demanding that $F_\perp$ [see Eq. (52)] is real valued. In the figure to the left P_1 and P_1' values are averaged over 1 to 6 GeV^2 using heavy-to-light form factors at large recoil (see Sec. IV A), and in the figure to the right we have used P_1 and P_1' values averaged over 16 to 19 GeV^2 using heavy-to-light form factors at low recoil (see Sec. IV B). Inside the triangles, the solid (black) lines correspond to the $F_\perp$ values; the dashed (blue) lines correspond to the C_{10} values as function of F_L and A_{FB}.

$$1 + \frac{\mathsf{P}_1^2 + \mathsf{P}_1'^2 + R^2(\mathsf{P}_1 - \mathsf{P}_1')^2 - (\mathsf{P}_1 - \mathsf{P}_1')\sqrt{R^2+1}\sqrt{R^2(\mathsf{P}_1 - \mathsf{P}_1')^2 + (\mathsf{P}_1' + \mathsf{P}_1)^2}}{2\mathsf{P}_1^2\mathsf{P}_1'^2} \le \frac{1-F_L}{F_\perp}$$
$$\le 1 + \frac{\mathsf{P}_1^2 + \mathsf{P}_1'^2 + R^2(\mathsf{P}_1 - \mathsf{P}_1')^2 + (\mathsf{P}_1 - \mathsf{P}_1')\sqrt{R^2+1}\sqrt{R^2(\mathsf{P}_1 - \mathsf{P}_1')^2 + (\mathsf{P}_1' + \mathsf{P}_1)^2}}{2\mathsf{P}_1^2\mathsf{P}_1'^2}. \qquad (55)$$

The constraint implied by this bound is depicted in Figs. 3 and 4 where we have considered two different values corresponding to different bins of averaged q^2 values. P_1 and P_1' are averaged over the q^2 region as described in the figure caption. The reader will note the rigorous constraint within the standard model, i.e., $R = -1$, depicted in the figures by the diagonal thick solid (blue) line that predicts $F_\perp$ to lie in a very narrow region, well approximated by a line that is a function of F_L and with the slope depending on the domain of q^2. It is obvious from Eq. (55) that as R^2 increases from unity, a wider region around this solid line is allowed. The allowed F_L-$F_\perp$ parameter space for

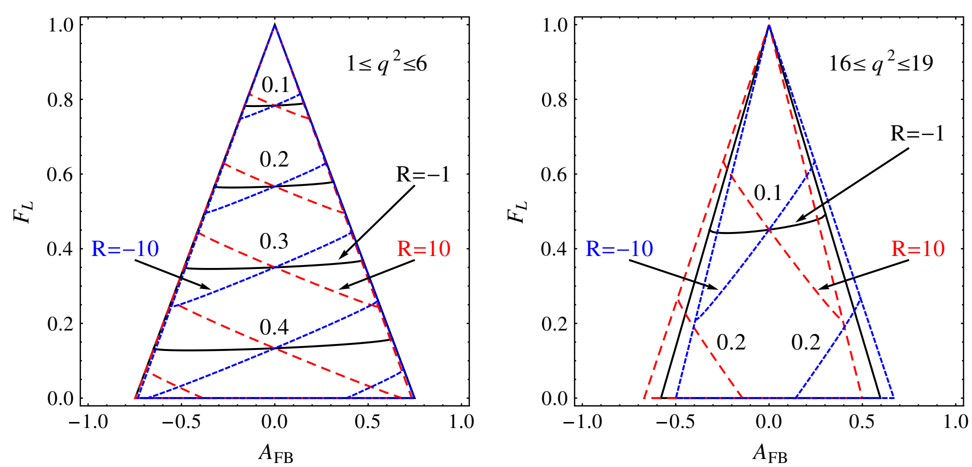

FIG. 2 (color online). The same as Fig. 1, except that the variation of the parameter space is studied as a function of R. The large-dashed (red) triangle and the identical lines correspond to $R = 10$. The $R = -10$ case is depicted by the small dashed (blue) line. $R = -1$ case is shown for reference with solid (black) lines. In the figure to the left P_1 and P_1' values are averaged over 1 to 6 GeV^2 and in the figure to the right we have used P_1 and P_1' values averaged over 16 to 19 GeV^2.

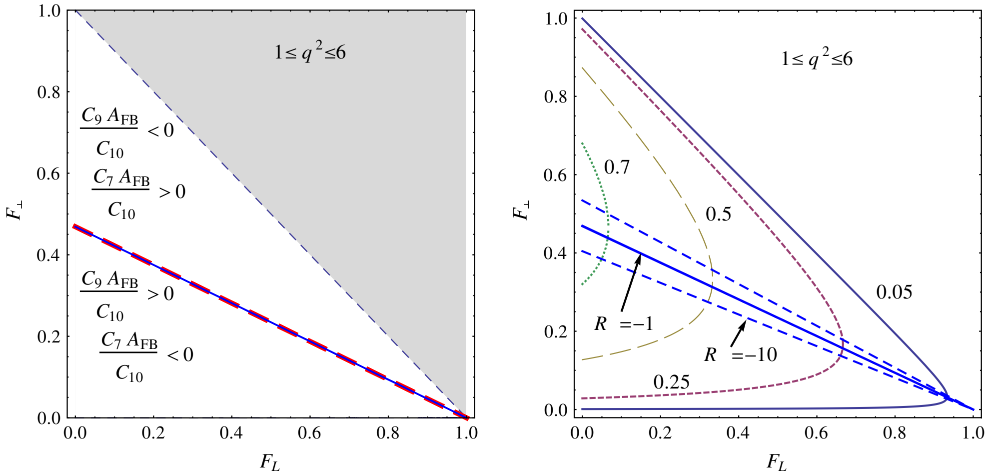

FIG. 3 (color online). The constraints on $F_L - F_\perp$ parameter space arising from Eq. (55) with the value of P_1 and P_1' averaged over 1 GeV$^2 \le q^2 \le 6$ GeV^2. The allowed region for $R = -1$ is depicted by the diagonal thick solid (blue) line that predicts $F_\perp$ to lie in a very narrow region, well approximated by a line. The allowed $F_L - F_\perp$ parameter space for $|R| = 10$ is also depicted as a wedge of dashed (blue) lines. The shaded region in the left figure is forbidden by $F_L + F_\perp + F_\parallel = 1$. In the figure on the left the thick dashed (red) line correspond to the solution of $F_\perp$ from Eq. (54) for $A_{\rm FB} = 0$. This line divides the allowed domain into two regions fixing the sign of $A_{\rm FB}$ relative to C_9/C_{10} and C_7/C_{10} as depicted in the figure. The additional cures in the right figure correspond to the constraint on $F_L - F_\perp$ arising from $Z_1^2 > 0$ for different values of $A_{\rm FB}$: 0.05, 0.25, 0.5, 0.7, where all the regions to the left of these curves are allowed.

$|R| = 10$ are also depicted as a wedge of dashed (blue) lines. In Fig. 4 on the right we have shown an enlarged region where for $|R| = 10$ we have plotted the values of $A_{\rm FB}$ evaluated using Eq. (54). As the figures shows, the $F_L - F_\perp$ correlation is not particularly sensitive to R. Also plotted in these figures are the constraints on the $F_L - F_\perp$ parameter space arising from $Z_1^2 > 0$ for different values of $A_{\rm FB}$. The plots also include other details which will be discussed later.

It is interesting to note that irrespective of the value of R, in the limit $\mathsf{P}_1' \to \mathsf{P}_1$ one obtains $(1 - F_L)/F_\perp = 1 + 1/\mathsf{P}_1^2$. In the limit $m_B \to \infty$ and the energy of the K^*, $E_{K^*} \to \infty$, it is easy to see that $\mathsf{P}_1 = \mathsf{P}_1' \to -1$, and we find that $F_\parallel = F_\perp$. In this limit Eq. (18) will result in a constant distribution in ϕ. Since P_1 and P_1' values differ slightly, we expect only a very small coefficient of $\cos\phi$.

The measurements of F_L and $F_\perp$ must be consistent with value of $A_{\rm FB}$ and there exists a domain of R, P_1, and

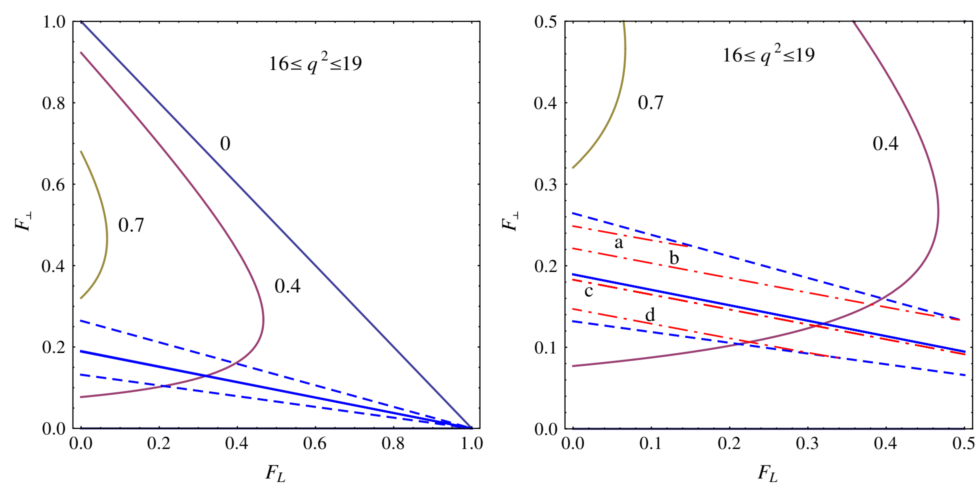

FIG. 4 (color online). The same as in Fig. 3 except that P_1 and P_1' averaged over 16 GeV$^2 \le q^2 \le 19$ GeV^2. The figure to the right is the inset of the figure to the left. In this figure the solid and the dashed diagonal (blue) lines are the same as in the figure to the right. The dotted-dashed (red) lines labeled by "a,b,c,d" correspond to $A_{\rm FB} = 0.5, 0.3, 0, -0.3$, respectively, for $R = -10$. The line "c" (for $A_{\rm FB} = 0$) divides the domain and corresponds to the thick dashed (red) line in Fig. 3. The $A_{\rm FB}$, F_L, and $F_\perp$ must be consistent as shown by the dotted-dashed lines. For $R = -1$, similar lines exist for different value of $A_{\rm FB}$ but overlap with the solid blue line. Hence, they are not depicted in the figure.

P_1' for which the consistency may hold. These values must be verified to be consistent with the values of observables. Bounds on P_1^2 can be obtained from the equations derived so far, in terms of observables alone. Extremizing P_1^2 in terms of all the nonobservables in Eq. (42), we can get following bounds on P_1^2:

$$\mathsf{P}_1^2 \lessgtr \frac{4F_\parallel F_\perp - \frac{16}{9}A_{\rm FB}^2}{F_\parallel^2} \quad \forall\ F_\parallel F_\perp \lessgtr \frac{2}{7}\left(\frac{4A_{\rm FB}}{3}\right)^2. \tag{56}$$

For $A_{\rm FB}=0$, we have already noted the exact equality $\mathsf{P}_1^2 = F_\perp/F_\parallel$. Analytical bounds on P_1' are also possible but are harder to obtain.

We now derive some useful relations that involve C_7 and are hence valid only at the leading order. Equations (42) and (47) can be reexpressed in this limit as

$$\frac{C_7}{C_{10}} = \frac{3}{2}\frac{\mathcal{F}_\parallel}{\mathcal{G}_\parallel}\frac{(\mathsf{P}_1^2F_\parallel - F_\perp)}{A_{\rm FB}(\mathsf{P}_1 - \mathsf{P}_1')} \tag{57}$$

where we have used the fact that $\tilde{\mathcal{G}}_\parallel = C_7\mathcal{G}_\parallel$ at leading order. We emphasize that C_7/C_{10} is not as clean as C_9/C_{10}, which is expressed in Eq. (51) in terms of observables and ratios of two form factors which are predicted exactly in heavy quark effective theory. C_7/C_{10} on the other hand depends on $\mathcal{F}_\parallel/\mathcal{G}_\parallel$ which in turn depends on the heavy quark effective theory form factor $\xi_\perp$. It may nevertheless be noted that the sign of $\mathcal{F}_\parallel/\mathcal{G}_\parallel$ is quite accurately predicted to be negative, since $A_1(q^2)$ and $T_2(q^2)$ are always positive. Equation (57) directly implies a constraint on the sign of C_7/C_{10}. It is easy to conclude that $(C_7/C_{10})A_{\rm FB} \gtrless 0$ only if $\mathsf{P}_1^2 \lessgtr F_\perp/F_\parallel$ when $\mathsf{P}_1 - \mathsf{P}_1' > 0$. Equation (56) together with Eq. (57) can be used to obtain more useful bounds that are purely in terms of observables alone, albeit they are not completely exhaustive. Equation (56) implies

$$\mathsf{P}_1^2F_\parallel - F_\perp \lessgtr \frac{Z_1 - F_\parallel F_\perp}{F_\parallel} \quad \forall\ F_\parallel F_\perp \lessgtr \frac{2}{7}\left(\frac{4A_{\rm FB}}{3}\right)^2, \tag{58}$$

which, in turn, implies for $(\mathsf{P}_1^2F_\parallel - F_\perp) < 0$ that

$$\frac{C_7}{C_{10}}A_{\rm FB} > 0 \quad \forall\ F_\parallel F_\perp < \frac{32}{63}A_{\rm FB}^2. \tag{59}$$

If, however, $(P^2F_\parallel - F_\perp) > 0$, we obtain an analogous condition

$$\frac{C_7}{C_{10}}A_{\rm FB} < 0 \quad \forall\ F_\parallel F_\perp > \frac{16}{27}A_{\rm FB}^2. \tag{60}$$

The above bounds have nothing to say on the sign of C_7/C_{10} in the region,

$$\frac{32}{63}A_{\rm FB}^2 \le F_\parallel F_\perp \le \frac{16}{27}A_{\rm FB}^2 \tag{61}$$

and may not be particularly useful, in general. One can nevertheless draw conclusions on the signs of the Wilson coefficients by combining Eq. (51) together with Eq. (57) to write

$$\left(\frac{2}{3}\frac{C_9}{C_{10}}\mathsf{P}_1'' - \frac{4}{3}\frac{C_7}{C_{10}}\mathsf{P}_1\right)A_{\rm FB} = (\mathsf{P}_1{}^2F_\parallel + F_\perp + \mathsf{P}_1Z_1) > 0, \tag{62}$$

where $\mathsf{P}_1'' = (\mathcal{G}_\parallel/\mathcal{F}_\parallel)(\mathsf{P}_1 + \mathsf{P}_1') > 0$ since each of $(\mathcal{G}_\parallel/\mathcal{F}_\parallel)$, P_1 and P_1' are always negative. Defining

$$E_1 \equiv \frac{C_9}{C_{10}}A_{\rm FB}, \qquad E_2 \equiv \frac{C_7}{C_{10}}A_{\rm FB}, \tag{63}$$

for convenience, Eq. (62) reads

$$\frac{2}{3}\mathsf{P}_1''E_1 - \frac{4}{3}\mathsf{P}_1E_2 > 0. \tag{64}$$

In SM, $C_7/C_{10} > 0$ and $C_9/C_{10} < 0$, hence, the sign of E_2 (E_1) will be same (opposite) to that observed for $A_{\rm FB}$. If for any q^2 we find $A_{\rm FB} > 0$, Eq. (64) cannot be satisfied unless the contribution from the E_2 term exceeds the E_1 term, or the sign of the E_2 term is wrong in SM. In the SM the E_2 term dominates at large recoil, i.e., small q^2, hence, $A_{\rm FB}$ must be positive at small q^2 to be consistent with SM. If $A_{\rm FB} < 0$ is observed for all q^2, i.e., no zero crossing of $A_{\rm FB}$ is seen, one can convincingly conclude that $C_7/C_{10} < 0$ in contradiction with SM. However, if zero crossing of $A_{\rm FB}$ is confirmed with $A_{\rm FB} > 0$ at small q^2 it is possible to conclude that the signs $C_7/C_{10} > 0$ and $C_9/C_{10} < 0$ are in conformity with SM, as long as other constraints like $Z_1^2 > 0$ hold. In Ref. [16] the zero crossing is indeed seen. However, in the $2\ {\rm GeV}^2 \le q^2 \le 4.3\ {\rm GeV}^2$ bin, $Z_1^2 > 0$ is only marginally satisfied. We emphasize that these conclusions drawn from Eq. (62) are exact and not altered by any hadronic uncertainties.

As mentioned in the text earlier, there are three sets of solutions of Wilson coefficient, C_9 and C_{10} and the effective photon vertices $\tilde{\mathcal{G}}_0$ and $\tilde{\mathcal{G}}_0 + \tilde{\mathcal{G}}_\parallel$. We next discuss the second and the third sets of solutions. The method of solutions is identical to first set of solutions [see Eqs. (41), (46), and (47)] and has been discussed in Appendix A. Using Eqs. (24b), (24c), and (24e), we can easily solve for $r_0 + r_\perp$ as

$$r_0 + r_\perp = \pm\frac{\sqrt{\Gamma_f}}{\sqrt{2}\mathcal{F}_\perp}(\mathsf{P}_2^2F_L + F_\perp \pm \mathsf{P}_2Z_2)^{1/2}, \tag{65}$$

where we have defined

$$Z_2 = \sqrt{4F_LF_\perp - \frac{32}{9}A_5^2}, \tag{66}$$

and the form factor ratios P^2 has been previously defined in Eq. (25). It is easy to derive that

$$r_0 + r_\perp|_{A_5=0} = \pm\frac{\sqrt{\Gamma_f}}{\sqrt{2}\mathcal{F}_\perp}(\sqrt{F_\perp} \pm \mathsf{P}_2\sqrt{F_L}) = 0, \tag{67}$$

since Eq. (24e) implies that we have $r_0 + r_\perp = 0$ at $A_5 = 0$. Once again, repeating the arguments made when $A_{\rm FB} = 0$, the expression of $r_0 + r_\perp = 0$ is valid for all values of the observables. The right-hand side of Eq. (67) can be zero only when positive sign ambiguity is chosen, since P^2 is negative. At the zero crossing points of A_5 we also have the following exact equality:

$$\mathsf{P}_2 = -\frac{\sqrt{F_\perp}}{\sqrt{F_L}}\bigg|_{A_5=0} \tag{68}$$

enabling measurements of form factor ratio P_2 in terms of observables, as long as the zero crossing of A_5 occurs in the large recoil region (we have verified at leading order that this is indeed true). We now write the second set of solutions of Wilson coefficients C_9 and C_{10} and the effective photon vertex $\tilde{\mathcal{G}}_0$:

$$C_{10} = \frac{\sqrt{\Gamma_f}}{\sqrt{2}\mathcal{F}_0}\frac{2}{3}\frac{\sqrt{2}A_5}{[\pm\sqrt{\mathsf{P}_2^2F_L + F_\perp + \mathsf{P}_2Z_2}]}, \tag{69}$$

$$C_9 = \frac{\sqrt{\Gamma_f}}{\sqrt{2}\mathcal{F}_0}\frac{(F_L\mathsf{P}_2\mathsf{P}_2' - F_\perp) - \frac{1}{2}(\mathsf{P}_2 - \mathsf{P}_2')Z_2}{[\pm(\mathsf{P}_2 - \mathsf{P}_2')\sqrt{\mathsf{P}_2^2F_L + F_\perp + \mathsf{P}_2Z_2}]}, \tag{70}$$

$$\tilde{\mathcal{G}}_0 = \frac{\sqrt{\Gamma_f}}{\sqrt{2}}\frac{(\mathsf{P}_2^2F_L - F_\perp)}{[\pm(\mathsf{P}_2 - \mathsf{P}_2')\sqrt{\mathsf{P}_2^2F_L + F_\perp + \mathsf{P}_2Z_2}]}. \tag{71}$$

It is easy to derive these relations which are identical to the ones derived in Eqs. (42), (46), and (47) except for the replacements: $F_\parallel \to F_L$, $A_{\rm FB} \to \sqrt{2}A_5$, $\mathcal{F}_\parallel \to \mathcal{F}_0$, $\mathcal{G}_\parallel \to \mathcal{G}_0$, which also imply that $r_\parallel \to r_0$, $\mathsf{P}_1 \to \mathsf{P}_2$, and $\mathsf{P}_1' \to \mathsf{P}_2'$. Straightforward extremization with respect to all the non-observables in Eq. (69) gives the following bounds on the form factor ratios P_2:

$$\mathsf{P}_2^2 \leqslant \frac{4F_LF_\perp - \frac{32}{9}A_5^2}{F_L^2} \quad \forall\ F_LF_\perp \leqslant \frac{2}{7}\left(\frac{4\sqrt{2}A_5}{3}\right)^2$$

Equations (69)–(71) give

$$\frac{C_9}{C_{10}} = \frac{2(F_L\mathsf{P}_2\mathsf{P}_2' - F_\perp) - (\mathsf{P}_2 - \mathsf{P}_2')Z_2}{\frac{4}{3}\sqrt{2}A_5(\mathsf{P}_2 - \mathsf{P}_2')}, \tag{72}$$

$$\frac{\tilde{\mathcal{G}}_0}{C_{10}} = \frac{3}{2}\mathcal{F}_0\frac{(\mathsf{P}_2^2F_L - F_\perp)}{\sqrt{2}A_5(\mathsf{P}_2 - \mathsf{P}_2')}. \tag{73}$$

Equation (72) can be inverted to obtain expressions for A_5 akin to the expression for $A_{\rm FB}$ obtained in Eq. (54). One easily derives

$$\sqrt{2}A_5 = \frac{3(RX_2 - \sqrt{Y_2(\mathsf{P}_2 - \mathsf{P}_2')^2(1+R^2) - X_2^2})}{4(\mathsf{P}_2 - \mathsf{P}_2')(1+R^2)}, \tag{74}$$

where $X_2 = 2(F_L\mathsf{P}_2\mathsf{P}_2' - F_\perp)$ and $Y_2 = 4F_LF_\perp$. Equations (72) and (73) can be combined to obtain

$$\left(\frac{2}{3}\frac{C_7}{C_{10}}\mathsf{P}_2'' - \frac{4}{3}\frac{C_9}{C_{10}}\mathsf{P}_2\right)A_5 = \frac{(\mathsf{P}_2^2F_L + F_\perp + \mathsf{P}_2Z_2)}{\sqrt{2}} > 0, \tag{75}$$

where $\mathsf{P}_2'' = (\mathcal{G}_0/\mathcal{F}_0)(\mathsf{P}_2 + \mathsf{P}_2') > 0$, since $\mathcal{G}_0/\mathcal{F}_0$, P_2, and P_2' are all negative. While this is not easily seen as in the case of P_1'' we have numerically verified at leading order that this is true for the entire q^2 domain. We have shown earlier by doing a power expansion in $A_{\rm FB}$, that $(\mathsf{P}_2^2F_L + F_\perp + \mathsf{P}_2Z_2)$ is always positive. It is easy to see that similar arguments can be made for the positivity of $(\mathsf{P}_2^2F_L + F_\perp + \mathsf{P}_2Z_2)$ by considering expansions in A_5. Hence, if the term in the bracket must be positive, A_5 must be positive. At large recoil the term in the bracket is expected to be positive.

The arguments made above for $r_0 + r_\perp$ can be repeated for $r_\wedge + r_\perp$. One easily solves using Eqs. (24b), (24d), and (24g):

$$r_\wedge + r_\perp = \pm\frac{\sqrt{\Gamma_f}}{\sqrt{2}\mathcal{F}_\perp}(\mathsf{P}_3^2(F_L + F_\parallel + \sqrt{2}\pi A_4) + F_\perp \pm \mathsf{P}_3Z_3)^{1/2}, \tag{76}$$

where P_3 has been defined in Eq. (25) and we have defined

$$Z_3 = \sqrt{4(F_L + F_\parallel + \sqrt{2}\pi A_4)F_\perp - \frac{16}{9}(A_{\rm FB} + \sqrt{2}A_5)^2}. \tag{77}$$

Equation (24g) implies that $r_\wedge + r_\perp = 0$ when $A_{\rm FB} + \sqrt{2}A_5 = 0$, hence,

$$\begin{aligned} r_\wedge + r_\perp|_{A_{\rm FB}+\sqrt{2}A_5=0} &= \pm\frac{\sqrt{\Gamma_f}}{\sqrt{2}\mathcal{F}_\perp}(\sqrt{F_\perp} \\ &\quad \pm \mathsf{P}_3\sqrt{F_L + F_\parallel + \sqrt{2}\pi A_4}) \\ &= 0. \end{aligned} \tag{78}$$

Once again we choose the positive sign to fix the sign ambiguity since P_3 is negative. At the zero crossing points of $A_{\rm FB} + \sqrt{2}A_5$ we, hence, have the equality

$$\mathsf{P}_3 = -\frac{\sqrt{F_\perp}}{\sqrt{F_L + F_\perp + \sqrt{2}\pi A_4}}\bigg|_{A_{\rm FB}+\sqrt{2}A_5=0}. \tag{79}$$

Hence, the zero crossing of $A_{\rm FB} + \sqrt{2}A_5$ enables the measurement of form factor ratio P_3 as well, in terms of observables. Note, however, that P_3 is not independent and related to P_1 and P_2 [see Eq. (25)]. The consequences of this relation will be discussed later. The new solutions to C_{10}, C_9 and $\tilde{\mathcal{G}}_\parallel + \tilde{\mathcal{G}}_0$:

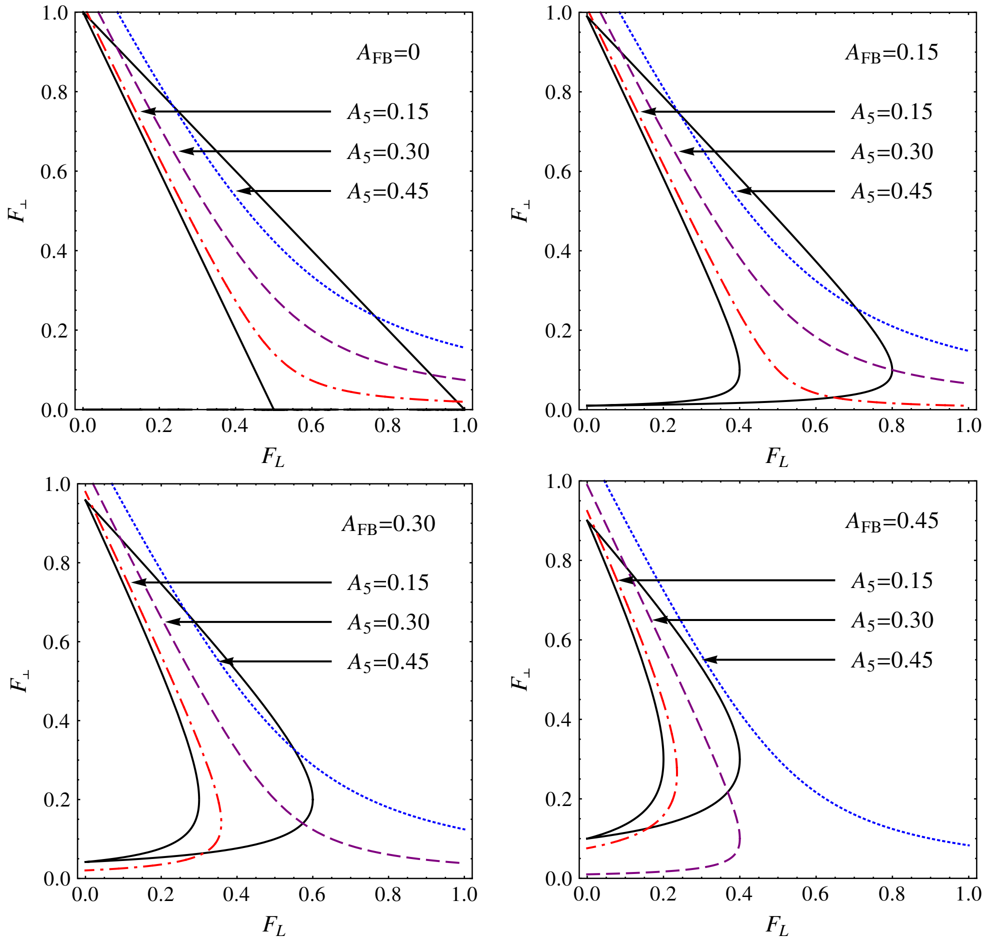

FIG. 5 (color online). The requirement that Z_1, Z_2, Z_3 must be real, for any consistent set of independent observables $A_{\rm FB}$, F_L, $F_\perp$, and A_5 constrains the allowed $F_L - F_\perp$ parameter space to lie only within the solid black lines. A_4 is given by Eq. (97). Even within the allowed $F_L - F_\perp$ domain only the region on the right is allowed depending on the values of $A_{\rm FB}$ and A_5. In the four figures we have sampled values of $A_{\rm FB}$ and A_5, which are as depicted. There is no hadronic assumption made in obtaining the constraints depicted in these plots.

$$C_{10} = \frac{\sqrt{\Gamma_f}}{\sqrt{2}(\mathcal{F}_0 + \mathcal{F}_\parallel)}\frac{2}{3}\frac{A_{FB} + \sqrt{2}A_5}{[\pm\sqrt{\mathsf{P}_3^2(F_L + F_\parallel + \sqrt{2}\pi A_4) + F_\perp + \mathsf{P}_3 Z_3}]}, \tag{80}$$

$$C_9 = \frac{\sqrt{\Gamma_f}}{\sqrt{2}(\mathcal{F}_0 + \mathcal{F}_\parallel)}\frac{((F_L + F_\parallel + \sqrt{2}\pi A_4)\mathsf{P}_3\mathsf{P}_3' - F_\perp) - \frac{1}{2}(\mathsf{P}_3 - \mathsf{P}_3')Z_3}{[\pm\sqrt{\mathsf{P}_3^2(F_L + F_\parallel + \sqrt{2}\pi A_4) + F_\perp + \mathsf{P}_3 Z_3}]}, \tag{81}$$

$$\tilde{\mathcal{G}}_\parallel + \tilde{\mathcal{G}}_0 = \frac{\sqrt{\Gamma_f}}{\sqrt{2}}\frac{(\mathsf{P}_3^2(F_L + F_\parallel + \sqrt{2}\pi A_4) - F_\perp)}{[\pm(\mathsf{P}_3 - \mathsf{P}_3')\sqrt{\mathsf{P}_3^2(F_L + F_\parallel + \sqrt{2}\pi A_4) + F_\perp + \mathsf{P}_3 Z_3}]}. \tag{82}$$

While these solutions may look more complicated they can also be obtained from Eqs. (42), (46), and (47) by the replacements $F_\parallel \to F_L + F_\parallel + \sqrt{2}\pi A_4$, $A_{\rm FB} \to A_{\rm FB} + \sqrt{2}A_5$, $\mathcal{F}_\parallel \to \mathcal{F}_\parallel + \mathcal{F}_0$, $\tilde{\mathcal{G}}_\parallel \to \tilde{\mathcal{G}}_\parallel + \tilde{\mathcal{G}}_0$, which also imply $r_\parallel \to r_\wedge$, $\mathsf{P}_1 \to \mathsf{P}_3$, and $\mathsf{P}_1' \to \mathsf{P}_3'$.

Once again straightforward extremization with respect to all the nonobservables in Eq. (80) results in the following bounds on the form factor ratio P_3:

$$\mathsf{P}_3^2 \leqslant \frac{4(F_L + F_\parallel + \sqrt{2}\pi A_4)F_\perp - \frac{16}{9}(A_{\rm FB} + \sqrt{2}A_5)^2}{(F_L + F_\parallel + \sqrt{2}\pi A_4)^2}$$

$$\forall\ (F_L + F_\parallel + \sqrt{2}\pi A_4)F_\perp \leqslant \frac{2}{7}\left(\frac{4(A_{\rm FB} + \sqrt{2}A_5)}{3}\right)^2.$$

These bounds are a very good test of our understanding of the form factors. Similar relations can be derived from Eqs. (80)–(82):

$$\frac{C_9}{C_{10}} = \frac{2((F_L + F_\parallel + \sqrt{2}\pi A_4)\mathsf{P}_3\mathsf{P}'_3 - F_\perp) - (\mathsf{P}_3 - \mathsf{P}'_3)Z_3}{\frac{4}{3}(A_{\mathrm{FB}} + \sqrt{2}A_5)(\mathsf{P}_3 - \mathsf{P}'_3)}, \tag{83}$$

$$\frac{\tilde{\mathcal{G}}_\parallel + \tilde{\mathcal{G}}_0}{C_{10}} = \frac{3}{2}(\mathcal{F}_\parallel + \mathcal{F}_0) \times \frac{(\mathsf{P}_3^2(F_L + F_\parallel + \sqrt{2}\pi A_4) - F_\perp)}{(A_{\mathrm{FB}} + \sqrt{2}A_5)(\mathsf{P}_3 - \mathsf{P}'_3)}. \tag{84}$$

Equation (83) can be inverted to obtain expressions for $A_{\mathrm{FB}} + \sqrt{2}A_5$ akin to the expression for A_{FB} obtained in Eq. (54). One easily derives

$$A_{\mathrm{FB}} + \sqrt{2}A_5 = \frac{3(RX_3 - \sqrt{Y_3(\mathsf{P}_3 - \mathsf{P}'_3)^2(1 + R^2) - X_3^2})}{4(\mathsf{P}_3 - \mathsf{P}'_3)(1 + R^2)} \tag{85}$$

where $X_2 = 2(F_L\mathsf{P}_3\mathsf{P}'_3 - F_\perp)$, $Y_2 = 4F_LF_\perp$, $X_3 = 2((F_L + F_\parallel + \sqrt{2}\pi A_4)\mathsf{P}_3\mathsf{P}'_3 - F_\perp)$, and $Y_3 = 4(F_L + F_\parallel + \sqrt{2}\pi A_4)F_\perp$.

From Eqs. (83) and (84) we can obtain yet another important relation, which is of the same kind as we obtained earlier in Eqs. (62) and (75):

$$\left(\frac{2}{3}\frac{C_7}{C_{10}}\mathsf{P}''_3 - \frac{4}{3}\frac{C_9}{C_{10}}\mathsf{P}_3\right)(A_{\mathrm{FB}} + \sqrt{2}A_5) = [(\mathsf{P}_3^2(F_L + F_\parallel + \sqrt{2}\pi A_4) + F_\perp + \mathsf{P}_3Z_3] > 0, \tag{86}$$

where $\mathsf{P}''_3 = (\mathcal{G}_0 + \mathcal{G}_\parallel)/(\mathcal{F}_0 + \mathcal{F}_\parallel)(\mathsf{P}_3 + \mathsf{P}'_3) > 0$. This is easily verified to be true at leading order for the entire q^2 domain. We have shown earlier by doing a power expansion in A_{FB} and A_5, that, respectively, $(\mathsf{P}_1^2F_\parallel + F_\perp + \mathsf{P}_1Z_1)$ and $(\mathsf{P}_2^2F_L + F_\perp + \mathsf{P}_2Z_2)$ are always positive. It is easy to see that similar arguments can be made for the positivity of $(\mathsf{P}_3^2(F_L + F_\parallel + 2\sqrt{2}\pi A_4) + F_\perp + \mathsf{P}_3Z_3)$ by considering expansions in $A_{\mathrm{FB}} + \sqrt{2}A_5$. These equations are equally useful to determine the sign of C_7 as discussed earlier; however, the form factors involved are not completely free from HQET form factor.

Equations (69)–(71) and (80)–(82) have been expressed in terms of from factor ratios P_2, P'_2, P_3, P'_3, which are not completely free from the hadronic form factors, both at large and at low recoil. The form factor ratios P_1 and P'_1 on the other hand is completely free from the Isgur-Wise form factors $\xi_\parallel$ and $\xi_\perp$ in the limit of heavy quark and large recoil of the vector meson. We can express the form factor ratios P_2, P'_2, P_3, P'_3 in terms of P_1 and P'_1. Equating the relations obtained for C_9/C_{10} and C_7/C_{10} in Eqs. (51) and (57) with those in Eqs. (72) and (73), we obtain relations only between form factor ratios P_1, P'_1, P_2, P'_2 and observables. The two equations so obtained can be used to solve for P_1 and P'_2 in terms of P_1 and P'_1.

$$\mathsf{P}_2 = \frac{2\mathsf{P}_1A_{\mathrm{FB}}F_\perp}{\sqrt{2}A_5(2F_\perp + Z_1\mathsf{P}_1) - Z_2\mathsf{P}_1A_{\mathrm{FB}}}, \tag{87}$$

$$\mathsf{P}'_2 = \frac{\sqrt{2}A_5(F_\perp - F_\parallel\mathsf{P}_1^2)\mathsf{P}_2^2\mathsf{P}'_1}{A_{\mathrm{FB}}T_2(\mathsf{P}_1 - \mathsf{P}'_1) + \sqrt{2}A_5(F_\perp - F_\parallel\mathsf{P}_1^2)\mathsf{P}_2\mathsf{P}'_1}, \tag{88}$$

where

$$T_2 = \mathsf{P}_1(F_\perp - F_L\mathsf{P}_2^2). \tag{89}$$

We emphasize that while P_2 and P'_2 on the left-hand side depend on the Isgur-Wise wave functions $\xi_\parallel$ and $\xi_\perp$, P_1 and P'_1 are independent of them. These two equations can be used to obtain information about the wave functions. Equation (87) is also very important in the sense that the domain of observables is itself constrained by the terms under the radical signs that must be positive to obtain real P_2. Similar relations for P_3 and P'_3 in terms of P_1 and P'_1 can be obtained by using Eqs. (51), (57), (83), and (84), to get

$$\mathsf{P}_3 = \frac{2\mathsf{P}_1A_{\mathrm{FB}}F_\perp}{(A_{\mathrm{FB}} + \sqrt{2}A_5)(2F_\perp + Z_1\mathsf{P}_1) - Z_3\mathsf{P}_1A_{\mathrm{FB}}}, \tag{90}$$

$$\mathsf{P}'_3 = \frac{(A_{\mathrm{FB}} + \sqrt{2}A_5)(F_\perp - F_\parallel\mathsf{P}_1^2)\mathsf{P}_3^2\mathsf{P}'_1}{A_{\mathrm{FB}}T_3(\mathsf{P}_1 - \mathsf{P}'_1) + \sqrt{2}A_5(F_\perp - F_\parallel\mathsf{P}_1^2)\mathsf{P}_3^2\mathsf{P}'_1}, \tag{91}$$

where

$$T_3 = \mathsf{P}_1[F_\perp(1 + \mathsf{P}_3^2) - \mathsf{P}_3^2(1 + \sqrt{2}\pi A_4)]. \tag{92}$$

As emphasized earlier, the Wilson coefficients are real constants except for the nonresonant regions. This implies that just like Z_1, both Z_2 and Z_3 are always real if resonant regions and CP violation are excluded:

$$4F_LF_\perp \geq \frac{16}{9}(\sqrt{2}A_5)^2, \tag{93}$$

$$4(F_L + F_\parallel + \sqrt{2}\pi A_4)F_\perp \geq \frac{16}{9}(A_{\mathrm{FB}} + \sqrt{2}A_5)^2. \tag{94}$$

The combination of bounds in Eqs. (44) and (93) results in yet another interesting bound among observables alone but involving only A_{FB}^2, A_5^2, and $F_\perp$:

$$4(1 - F_\perp)F_\perp \geq \frac{16}{9}(A_{\mathrm{FB}}^2 + 2A_5^2). \tag{95}$$

In Fig. 6 we depict the constraint on A_{FB}, A_5, and $F_\perp$ arrived at by Eq. (95). We emphasize that like the bounds derived in Eqs. (45), (93), and (94), this bound is also completely free from any hadronic uncertainty.

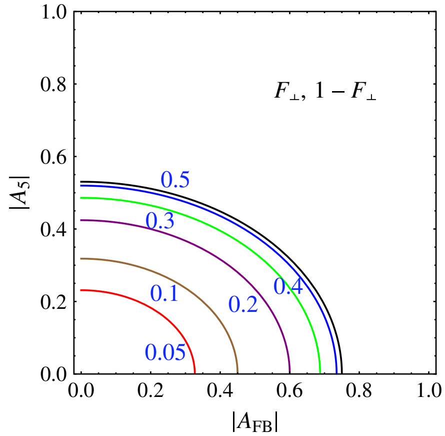

FIG. 6 (color online). The constraint on A_{FB}, A_5, and $F_\perp$ arrived at by Eq. (95). The depicted values correspond to both $F_\perp$ and $1-F_\perp$.

In Eq. (25) we showed that P_3 is not independent but related to P_1 and P_2. P_3 and P_2 are themselves expressed in terms of observables and P_1 in Eqs. (90) and (87), respectively. This constraint results in an interesting relation that depends on observables alone:

$$Z_3 = Z_1 + Z_2. \tag{96}$$

We use this relation to solve for A_4 leading to

$$A_4 = \frac{8A_5 A_{FB}}{9\pi F_\perp} + \sqrt{2}\frac{\sqrt{F_L F_\perp - \frac{8}{9}A_5^2}\sqrt{F_\parallel F_\perp - \frac{4}{9}A_{FB}^2}}{\pi F_\perp}. \tag{97}$$

Since $F_\perp$ is already predicted in Eq. (52) in terms of the already measured observables F_L and A_{FB} and P_1, P_1' and R, we can estimate A_4 in terms of A_5. The correlations predicted by Eq. (95) would have to hold unless NP contributes. In Figs. 7 and 8, we present the correlation between the observables. It may be noted that Eq. (97) is a relation involving only observables without any assumptions of hadronic form factors, hence, its violation must be an unambiguous signal of NP.

Let us summarize the approach that has led to these solutions. We have six observables, the decay width of $B \to K^*\ell^+\ell^-$, Γ_f, the helicity fractions F_L and $F_\perp$ and the angular asymmetries A_{FB}, A_4 and A_5. These six observables

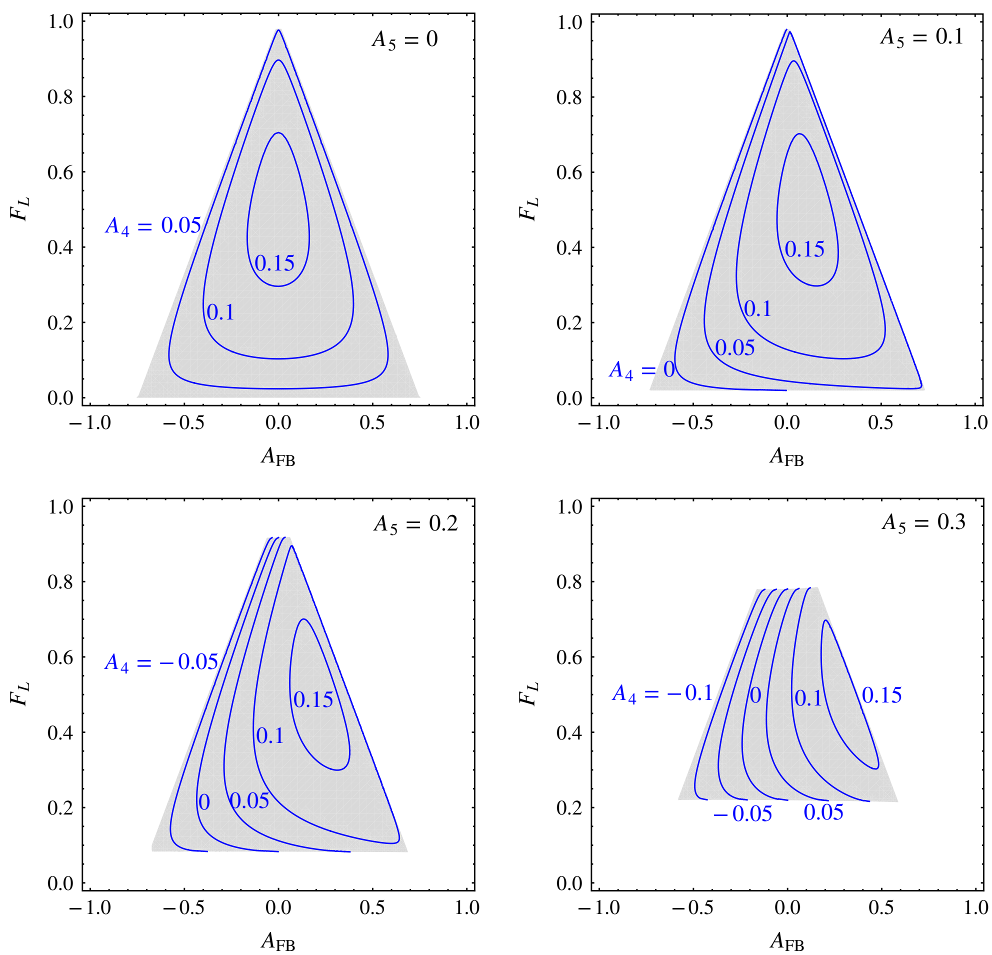

FIG. 7 (color online). The allowed region in the $F_L - F_\perp$ parameter space, shaded as gray, for $R = -1$ and different values of A_5. The values of P_1 and P_1' are averaged over 1 GeV$^2 \le q^2 \le 6$ GeV^2. The blue lines correspond to the value of A_4 that is estimated using Eq. (97).

are expressed in terms of eight theoretical parameters in the most general approach. The parameters being the six effective form factors $\mathcal{F}_0$, $\mathcal{F}_\parallel$, $\mathcal{F}_\perp$, $\tilde{\mathcal{G}}_0$, $\tilde{\mathcal{G}}_\parallel$, and $\tilde{\mathcal{G}}_\perp$ and the two Wilson coefficients C_9 and C_{10}. Three of the observables Γ_f, F_L, and $A_{\rm FB}$ have already been measured by several experiments. We assume three further inputs—the ratio $R = C_9/C_{10}$ as it is theoretically reliably estimated in SM and the ratios P_1 and P_1' of form factors as defined in Sec. IV. P_1 and P_1' are accurately predicted theoretically in the heavy quark limit to be free from higher order corrections and the known universal form factors $\xi_\parallel$ and $\xi_\perp$. These inputs allow us to estimate $F_\perp$. We find that by making an assumption of one further observable A_5, we are able to predict the only remaining observable A_4, completely free from hadronic parameters or estimate of R. Clearly, only five of the observables are independent in SM and $\mathcal{F}_\parallel$ remains unsolved given all the observables possible. It has also been realized earlier [38] following a different approach that there exist symmetries in the angular distribution which reduce the number of independent observables. We emphasize that in our approach, C_9/C_{10} and all the expressions independent of Wilson coefficients are "clean" in the large recoil limit.

VI. THE LOW-RECOIL LIMIT

In Sec. IV B we found that [see Eqs. (35) and (37)] in the low-recoil limit the form factors satisfied the conditions

$$\frac{\mathcal{G}_\parallel}{\mathcal{F}_\parallel} = \frac{\mathcal{G}_\perp}{\mathcal{F}_\perp} = \frac{\mathcal{G}_0}{\mathcal{F}_0} = \hat{\kappa},$$

which implies that

$$r_\parallel = r_\perp = r_0 = r_\wedge \equiv r.$$

This reduces the number of independent relations [see Eqs. (22a)–(22f)] and the low-recoil limit thus needs to be treated more carefully. In this limit the Wilson coefficients C_7 and C_9 cannot be solved following the approach in Appendix A, as it is obvious from Eq. (A8). We will, however, be able to solve for r and, in turn, for C_7 and C_9 if $\hat{\kappa}$ is assumed or equivalently with the additional input of $\mathcal{G}_\parallel$, since $\mathcal{F}_\parallel$ is in any case a required input. This results in one additional constraint relation between observables. In this section we derive a new relation among observables that will test the validity of the assumption on the form factors in the low-recoil limit. We will also elaborate on various other constraints in this limit.

We begin by considering Eqs. (A1)–(A3) in the low-recoil limit. Clearly, since $r^2 + C_{10}^2$ is independent of helicity, Eqs. (A1) and (A2) reduce to the same equation, hence, we have

$$r^2 + C_{10}^2 = \frac{\Gamma_f F_\parallel}{2\mathcal{F}_\parallel^2} = \frac{\Gamma_f F_\perp}{2\mathcal{F}_\perp^2} \equiv \frac{\hat{F}\Gamma_f}{2}, \tag{98a}$$

$$4rC_{10} = \frac{2A_{\rm FB}\Gamma_f}{3\mathcal{F}_\parallel\mathcal{F}_\perp} \equiv \frac{4A_{\rm FB}}{3\sqrt{F_\parallel F_\perp}}\frac{\hat{F}\Gamma_f}{2}, \tag{98b}$$

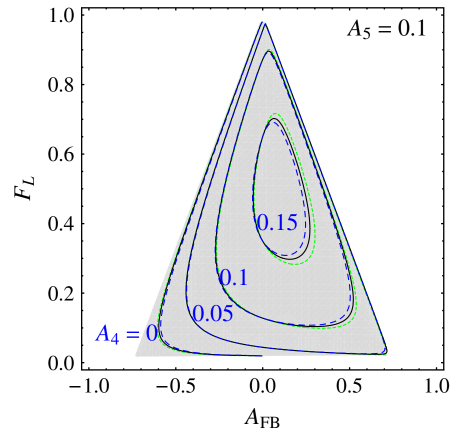

FIG. 8 (color online). The same as Fig. 7, but studying the variation in R. The small dashed (green) curves are for the case $R = 10$ while the big dashed (blue) curves correspond to $R = -10$. The solid black curves are for the standard model value of $R = -1$. Note the insensitivity to the value of R for the large recoil region 1 GeV$^2 \le q^2 \le 6$ GeV^2.

where

$$\hat{F} \equiv \frac{F_\parallel}{\mathcal{F}_\parallel^2} = \frac{F_\perp}{\mathcal{F}_\perp^2}. \tag{99}$$

Equation (50) then implies that

$$\mathsf{P}_1^2 = \mathsf{P}_1'^2 = \frac{F_\perp}{F_\parallel} = \frac{\mathcal{F}_\perp^2}{\mathcal{F}_\parallel^2}. \tag{100}$$

It is obvious from Eq. (98) that we can solve for r^2 and C_{10}^2:

$$r^2 = \frac{\hat{F}\Gamma_f}{4}\left(1 + \frac{Z_1}{\sqrt{2F_\parallel F_\perp}}\right), \tag{101}$$

$$C_{10}^2 = \frac{\hat{F}\Gamma_f}{4}\left(1 - \frac{Z_1}{\sqrt{2F_\parallel F_\perp}}\right). \tag{102}$$

The sign of r/C_{10} is fixed such that

$$\frac{r}{C_{10}} = \frac{3}{4}\frac{2\sqrt{F_\perp F_\parallel} + Z_1}{A_{\rm FB}}, \tag{103}$$

in order to satisfy the limit derived by appropriate combination of Eqs. (47) and (46).

In the low-recoil limit "r" is the same not just for $\parallel$ and $\perp$ helicities but for all three helicities. This requires, in analogy with Eq. (100), that

$$\mathsf{P}_1^2 = \mathsf{P}_1'^2 = \frac{F_\perp}{F_\parallel} = \frac{\mathcal{F}_\perp^2}{\mathcal{F}_\parallel^2}, \tag{104a}$$

$$\mathsf{P}_2^2 = \mathsf{P}_2'^2 = \frac{F_\perp}{F_L} = \frac{\mathcal{F}_\perp^2}{\mathcal{F}_0^2}, \tag{104b}$$

$$\mathsf{P}_3^2 = \mathsf{P}_3'^2 = \frac{F_\perp}{(F_L + F_\parallel)} = \frac{\mathcal{F}_\perp^2}{(\mathcal{F}_0^2 + \mathcal{F}_\parallel^2)}. \tag{104c}$$

One can, hence, measure P_1, P_2, and P_3 in the low-recoil region in terms of the ratio of helicity fractions. Hence, the value $C_{10}^2\mathcal{F}_\parallel^2$ can be expressed in terms of observables

TABLE IV. The form factor ratios P_1, P_1' and $\mathcal{F}_\parallel$ averaged over different q^2 bins at low recoil.

GeV^2	14.18–16	16–19
P_1	-0.6836	-0.4719
P_1'	-0.7093	-0.4952
$\mathcal{F}_\parallel(10^{-12})$	-27.8735	-25.0050

alone. In the large recoil case $C_{10}^2\mathcal{F}_\parallel^2$ depended on P_1 and P_2. The form factor $\mathsf{P}_1 = \mathsf{P}_1'$ can be measured, enabling a possibility of verifying the estimates presented in Table IV. To derive a relation between observables that is valid at low recoil and that tests the validity of the approximation, we note that Eq. (98) leads to the generalized relation

$$\frac{r^2 + C_{10}^2}{2rC_{10}} = \frac{2}{3}\frac{A_{\mathrm{FB}}}{\sqrt{F_\parallel F_\perp}} = \frac{2}{3}\frac{\sqrt{2}A_5}{\sqrt{F_L F_\perp}} = \frac{2}{3}\frac{(A_{\mathrm{FB}} + \sqrt{2}A_5)}{\sqrt{(1 - F_\perp + \sqrt{2}\pi A_4)F_\perp}}. \tag{105}$$

The equalities on the left side of the above equation yields two interesting relations

$$\sqrt{2}A_5 = A_{\mathrm{FB}}\frac{\sqrt{F_L}}{\sqrt{F_\parallel}}, \tag{106}$$

$$A_4 = \frac{\sqrt{2}}{\pi}\sqrt{F_L F_\parallel}. \tag{107}$$

It is easily seen by direct substitution of Eq. (106) in Eq. (97) that it reduces to Eq. (107), hence, it is not independent. It is emphasized that a reasonable validity of the low-recoil approximation requires large q^2 and not the exact equality of form factors as derived Eq. (104). Even though the values of the form factors depicted in Table IV are not exactly equal, the low-recoil approximation works well as seen from Fig. 9 where we plot the left-hand and right-hand sides of Eqs. (106) and (107). These figures demonstrate the domain of validity of the low-recoil approximation and the region where new physics can be tested. The values of observables are estimated using the form factors given in Table IV.

We emphasize that the relations derived in Eqs. (106) and (107) are extremely important both in testing the validity of the low-recoil approximation and the presence of new physics. The value of A_5 predicted by these relations tests the validity of the low-recoil approximation, whereas the value of A_4 verifies the validity of SM. If both the relations are found to be valid, it would prove both the validity of the low-recoil limit and the absence of new physics. On the other hand, if both the relations fail, we must conclude that low-recoil limit is not valid. The presence of new physics could still be tested by the validity of Eq. (97) even in this large q^2 domain. The remaining meaningful possibility is that Eq. (106) holds and (107) is violated. This would imply validity of low-recoil limit but signal the presence of new physics. It is interesting to note that one should expect from Eqs. (106) and (107) a very tiny product of asymmetries A_4 and A_5:

$$A_4 A_5 = \frac{A_{\mathrm{FB}}F_L}{\pi}, \tag{108}$$

since the right-hand side A_{FB} and F_L have already been measured. We emphasize that even in the low-recoil limit, C_9/C_{10} and all the expressions independent of Wilson coefficients are independent of the universal form factors $\xi_\parallel$ and $\xi_\perp$.

VII. CONCLUSIONS

In this paper we have derived several important new results. After a brief introduction, we discuss the differential decay distribution of $B \to K^*\ell^+\ell^-$ and introduced the

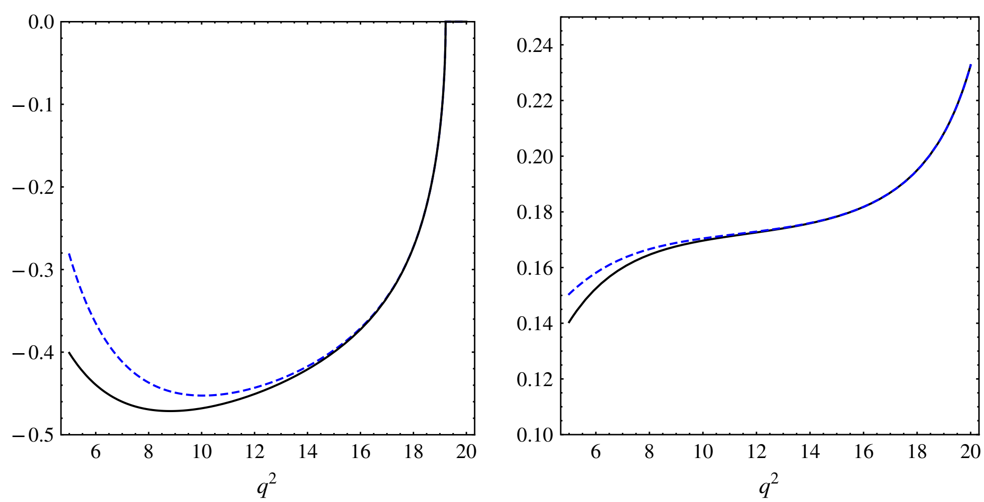

FIG. 9 (color online). In the figure to the left the left-hand side (solid curve) and right-hand side (dashed blue curve) of Eq. (106) are plotted. The figure on the right is the corresponding figure for Eq. (107). These figures demonstrate the domain of validity in q^2 for the low-recoil approximation and the region where new physics can be tested. The values are estimated using the form factors given in Table IV.

observables Γ_f, F_L, $F_\perp$, $A_{\rm FB}$, A_4, and A_5. While the partial decay rate Γ_f can be measured by angular integration, the other observables require a study of angular distributions. We showed how uniangular distributions in the azimuthal angle ϕ can be used to measure the helicity fraction $F_\perp$. F_L and $A_{\rm FB}$ have already been measured by studying the uniangular distribution in θ_ℓ. A_4 and A_5 can only be measured by a complete angular analysis involving θ_ℓ and ϕ requiring higher statistics. After setting up our notation and defining the observables in terms of form factors, we expressed the amplitude in the most general form within the standard model as $\mathcal{A}_\lambda^{L,R} = C_{L,R}\mathcal{F}_\lambda - \tilde{\mathcal{G}}_\lambda$, where $\lambda = \{0, \perp, \|\}$ is the helicity of the K^*, $C_{L,R} = C_9^{\rm eff} \mp C_{10}$ and L, R defines the chirality of the ℓ^-. The form factors $\mathcal{F}_\lambda$ and $\tilde{\mathcal{G}}_\lambda$ are expressed in terms of conventional $B \to K^*$ form factors V, $A_{1,2}$ and $T_{1,2,3}$. To be exact $\tilde{\mathcal{G}}_\lambda \equiv C_7\mathcal{G}_\lambda + \cdots$ with the dots representing the higher order and nonfactorizable contributions and only at leading order $\mathcal{G}_\lambda$'s are related to $T_{1,2,3}$. It may be noted that even at leading order C_7 and $\mathcal{G}_\lambda$ cannot be separated and C_7 can only be defined at leading order on assuming $\mathcal{G}_\lambda$. The six observables are thus defined in terms of eight parameters, the six form factors $\mathcal{F}_\lambda$, $\tilde{\mathcal{G}}_\lambda$ and two Wilson Coefficients $C_{9,10}$. Hence, only six theoretical parameters can be eliminated in terms of observables and a minimum of two reliable theoretical inputs are needed, to resolve between new physics and hadronic contributions. This is made possible by the significant advances in our understanding of form factors that permit us to make truly these reliable inputs. One of our achievements are derivations of "clean relations" that permit the verifications of these hadronic inputs.

The $B \to K^*$ form factors are estimated using heavy quark effective theory and the treatment varies on the recoil energy of the K^*. At large recoil the ratio of the form factors $\mathsf{P}_1 = \mathcal{F}_\perp/\mathcal{F}_\|$ and $\mathsf{P}_1' = \tilde{\mathcal{G}}_\perp/\tilde{\mathcal{G}}_\|$ are reliably evaluated at $\mathcal{O}(1/m_b)$ to be free from universal wave functions and are unaltered by nonfactorizable contributions and higher order corrections in α_s. In the large recoil limit we, therefore, choose P_1 and P_1' as the two inputs in addition to observables. In the low-recoil limit the relations $\mathsf{P}_1 = \mathsf{P}_1'$ between the form factors serves as an additional input.

We summarize briefly a few significant new results. The simple analytic derivation and solutions to the Wilson coefficients in terms of the observables and "clean" form factors was achieved by defining new variables $r_\lambda = \tilde{\mathcal{G}}_\lambda/\mathcal{F}_\lambda - C_9$. These enable solutions to C_9 and C_{10} in terms of observables, P_1, P_1' and the form factor $\mathcal{F}_\|$ to be

$$C_9 = \frac{\sqrt{\Gamma_f}}{\sqrt{2}\mathcal{F}_\|}\frac{(F_\|\mathsf{P}_1\mathsf{P}_1' - F_\perp) - \frac{1}{2}(\mathsf{P}_1 - \mathsf{P}_1')Z_1}{[\pm(\mathsf{P}_1 - \mathsf{P}_1')\sqrt{\mathsf{P}_1^2F_\| + F_\perp + \mathsf{P}_1Z_1}]},$$

$$C_{10} = \frac{\sqrt{\Gamma_f}}{\sqrt{2}\mathcal{F}_\|}\frac{2}{3}\frac{A_{\rm FB}}{[\pm\sqrt{\mathsf{P}_1^2F_\| + F_\perp + \mathsf{P}_1Z_1}]},$$

where Z_1 is expressed in terms of observables in Eq. (43). Two additional solutions for C_9 and C_{10} can be obtained in terms of different observables. These are obtained by the replacements

(i) $F_\| \to F_L$, $A_{\rm FB} \to \sqrt{2}A_5$, $\mathcal{F}_\| \to \mathcal{F}_0$, $\mathcal{G}_\| \to \mathcal{G}_0$, which also imply that $r_\| \to r_0$, $\mathsf{P}_1 \to \mathsf{P}_2$ and $\mathsf{P}_1' \to \mathsf{P}_2'$.

(ii) $F_\| \to F_L + F_\| + \sqrt{2}\pi A_4$, $A_{\rm FB} \to A_{\rm FB} + \sqrt{2}A_5$, $\mathcal{F}_\| \to \mathcal{F}_\| + \mathcal{F}_0$, $\mathcal{G}_\| \to \mathcal{G}_\| + \mathcal{G}_0$, which also imply $r_\| \to r_\wedge$, $\mathsf{P}_1 \to \mathsf{P}_3$ and $\mathsf{P}_1' \to \mathsf{P}_3'$.

We found that the form factor ratios P_1, P_2, and P_3 can be directly measured in terms of the ratio of helicity fractions at q^2 corresponding to the zero crossings of asymmetries $A_{\rm FB}$, A_5 and $A_{\rm FB} + \sqrt{2}A_5$, respectively, by the relations:

$$\mathsf{P}_1 = -\frac{\sqrt{F_\perp}}{\sqrt{F_\|}}\Bigg|_{A_{\rm FB}=0}, \qquad \mathsf{P}_2 = -\frac{\sqrt{F_\perp}}{\sqrt{F_L}}\Bigg|_{A_5=0},$$

$$\mathsf{P}_3 = -\frac{\sqrt{F_\perp}}{\sqrt{F_L + F_\perp + \sqrt{2}\pi A_4}}\Bigg|_{A_{\rm FB}+\sqrt{2}A_5=0}.$$

Since we have neglected the tiny CP violation in the standard model, we find that the observables must satisfy the following inequalities which are completely free from any hadronic uncertainties and hence clean. These relations are

$$4F_\|F_\perp \geq \frac{16}{9}A_{\rm FB}^2 \qquad 4F_LF_\perp \geq \frac{16}{9}(\sqrt{2}A_5)^2,$$

$$4(1 - F_\perp)F_\perp \geq \frac{16}{9}(A_{\rm FB}^2 + 2A_5^2),$$

$$4(F_L + F_\| + \sqrt{2}\pi A_4)F_\perp \geq \frac{16}{9}(A_{FB} + \sqrt{2}A_5)^2.$$

In Fig. 5 we have plotted the constraints on $F_L - F_\perp$ that depend only on observables. The condition $4F_\|F_\perp \geq 16/9A_{\rm FB}^2$ implies that if $|A_{\rm FB}|$ is large, F_L must be small so that $4F_\|F_\perp$ can be sufficiently large. Our approach is sensitive enough to already show tensions in the data [16].

Clearly, expressions for C_9 and C_{10} are not "clean." However, the ratio C_9/C_{10} is obtained as a "clean expression." Assuming the theoretical estimate of C_9/C_{10} which is reliably evaluated at next-to-next-to-leading logarithm in the standard model, we "cleanly" predicted $F_\perp$ in Eq. (52). The correlation between $A_{\rm FB}$, F_L, and $F_\perp$ have been plotted in Figs. 1–4. We showed that the valid domain of $A_{\rm FB}$ is constrained in terms of F_L as follows:

$$\frac{-3(1 - F_L)}{4}T_- \leq A_{FB} \leq \frac{3(1 - F_L)}{4}T_+,$$

where $T_\pm$ is given in terms of P_1, P_1' and R in Eq. (53). It is interesting to note that F_L and $F_\perp$ are constrained with the standard model to lie in a very narrow region, well approximated by a line as shown in Figs. 3 and 4. The effective photon vertex $\tilde{\mathcal{G}}_\|$ and $\tilde{\mathcal{G}}_0$ can also be expressed as a clean expression.

The C_9/C_{10} and C_7/C_{10} ratios in Eqs. (51) and (57) were combined to obtain

$$\left(\frac{2}{3}\frac{C_9}{C_{10}}\mathsf{P}_1'' - \frac{4}{3}\frac{C_7}{C_{10}}\mathsf{P}_1\right)A_{\mathrm{FB}} = (\mathsf{P}_1{}^2 F_\parallel + F_\perp + \mathsf{P}_1 Z) > 0.$$

If the A_{FB} zero crossing is confirmed [16] with $A_{\mathrm{FB}} > 0$ at small q^2, then based on the signs of the from factors, it is unambiguously concluded that the signs of C_7/C_{10} and C_9/C_{10} are in agreement with the standard model, i.e., $C_7/C_{10} > 0$ and $C_9/C_{10} > 0$ as long as other constraints like $Z_1^2 > 0$ hold. In Ref. [16] the zero crossing is indeed seen. However, in the $2\ \mathrm{GeV}^2 \le q^2 \le 4.3\ \mathrm{GeV}^2$ bin, $Z_1^2 > 0$ is only marginally satisfied. These conclusions are exact and not altered by any hadronic uncertainties.

We have obtained three sets of C_9/C_{10} and C_7/C_{10} solutions involving different observables and form factor ratios. Since, the form factor ratios P_1 and P_1' are the ones that are most reliably estimated in both large recoil and low-recoil limits, we obtain relations for P_2, P_2' and P_3, P_3' in terms of P_1, P_1' and observables. Equating the relations obtained for C_9/C_{10} and C_7/C_{10} in Eqs. (51) and (57) with those in Eqs. (72) and (73), we get

$$\mathsf{P}_2 = \frac{2\mathsf{P}_1 A_{\mathrm{FB}} F_\perp}{\sqrt{2}A_5(2F_\perp + Z_1\mathsf{P}_1) - Z_2\mathsf{P}_1 A_{\mathrm{FB}}},$$

$$\mathsf{P}_2' = \frac{\sqrt{2}A_5(F_\perp - F_\parallel \mathsf{P}_1^2)\mathsf{P}_2^2\mathsf{P}_1'}{A_{\mathrm{FB}}T_2(\mathsf{P}_1 - \mathsf{P}_1') + \sqrt{2}A_5(F_\perp - F_\parallel \mathsf{P}_1^2)\mathsf{P}_2\mathsf{P}_1'},$$

where $T_2 = \mathsf{P}_1(F_\perp - F_L\mathsf{P}_2^2)$. Similar relations can be derived for P_3 and P_3' [see Eqs. (90) and (91)]. Even though P_2, P_2' and P_3, P_3' inherently depend on $\xi_\parallel$ and $\xi_\perp$, we have expressed them in terms of "clean relations" above. Hence, in our approach, all the expressions for observables are "clean," with only the Wilson coefficients C_7, C_9, and C_{10} being expressed in terms of only one form factor $\mathcal{G}_\parallel$ or $\mathcal{F}_\parallel$.

We have derived significant constraints between observables that can be used to test for new physics. The constraint purely in terms of observables arises, since P_2 and P_3 are expressed in terms of observables and P_1 while P_3 itself is related in Eq. (25) to P_1 and P_2. We obtain the interesting constraint (97) among observables:

$$A_4 = \frac{8A_5A_{\mathrm{FB}}}{9\pi F_\perp} + \sqrt{2}\frac{\sqrt{F_LF_\perp - \frac{8}{9}A_5^2}\sqrt{F_\parallel F_\perp - \frac{4}{9}A_{\mathrm{FB}}^2}}{\pi F_\perp}.$$

The observables A_4 and A_5 also impose constraints on the parameter space. In Fig. 5 we plot constraints on the parameter space of $F_L - F_\perp$ that depend purely on observables A_{FB} and A_5 with A_4 being calculated in terms of the above relation between observables. As seen, the parameter space is highly constrained in the standard model.

We introduced six observables of which three Γ_f, F_L, and A_{FB} have already been measured. We showed that $F_\perp$ can expressed in terms of P_1, P_1' and the ratio C_9/C_{10}. If we further choose a value for A_5, A_4 can be obtained. In Fig. 7 we depict the constraints in the $A_{\mathrm{FB}} - F_L$ parameter space. These constraints and the constraints obtained in Fig. 1 completely fix the parameter space and predict the values of yet unmeasured observables.

We pay special attention to the low-recoil limit and derive two new relations

$$\sqrt{2}A_5 = A_{\mathrm{FB}}\frac{\sqrt{F_L}}{\sqrt{F_\parallel}}, \qquad A_4 = \frac{\sqrt{2}}{\pi}\sqrt{F_LF_\parallel} \tag{111}$$

in terms of observables alone. These two relations allow us to test not only the validity of the low-recoil approximation but also the presence of new physics. The value of A_5 predicted by these relations tests the validity of the low-recoil approximation, whereas the value of A_4 verifies the validity of SM. If both relations hold, we verify that the low-recoil approximation is correct and that no new physics can exist. If both relations fail, we can conclude that the low-recoil approximation fails but one can nevertheless still test for new physics by Eq. (97), which is valid in general. If A_5 is accurately predicted but A_4 does not have the value given by these two relations, one can conclude that there is new physics and that the low-recoil limit is accurate.

In this paper we reexamined the new physics discovery potential of the mode $B \to K^*\ell^+\ell^-$. This mode has an advantage as a multitude of observables can be measured via angular analysis. We showed how the multitude of related observables obtained from $B \to K^*\ell^+\ell^-$ can provide many new clean tests of the standard model and discriminate new physics contributions from hadronic effects. The hallmark of these tests is that most of them are independent of the unknown form factors $\xi_\parallel$ and $\xi_\perp$ in heavy quark effective theory. In the large recoil limit [at $\mathcal{O}(1/m_b)$] these relations are valid to all orders in α_s. We derive a relation between observables that is free of form factors and Wilson coefficients, the violation of which will be an unambiguous signal of new physics. We also obtained for the first time relations between observables and form factors that are independent of Wilson coefficients and enable verification of hadronic estimates. We show how form factor ratios can be measured directly from a helicity fraction without any assumptions whatsoever. We find that the allowed parameter space for observables is very tightly constrained in the standard model, thereby providing clean signals of new physics. We examine in detail both the large-recoil and low-recoil regions of the K^* meson and probe special features valid in the two limits. Another new relation involving only observables that would verify the validity of the relations between form factors assumed in the low-recoil region was also derived. The several relations and constraints derived will provide unambiguous signals of new physics if it contributes to these decays. We emphasize that in our approach, C_9/C_{10} and all the expressions independent of Wilson coefficients are clean in the large recoil limit, and in the low-recoil limit they are reliably calculated as they do not depend on the universal form factors $\xi_\parallel$ and $\xi_\perp$.

APPENDIX A: DERIVATION OF WILSON COEFFICIENTS

Below we present the solution of $r_\parallel + r_\perp$. The solutions of $r_0 + r_\perp$ and $r_\wedge + r_\perp$ are identical.

We start with the expression involving $r_\parallel$ and $r_\perp$ in terms of observables as expressed in Eqs. (24a), (24c), and (24f):

$$r_\parallel^2 + C_{10}^2 = \frac{F_\parallel \Gamma_f}{2\mathcal{F}_\parallel^2}, \tag{A1}$$

$$r_\perp^2 + C_{10}^2 = \frac{F_\perp \Gamma_f}{2\mathcal{F}_\perp^2}, \tag{A2}$$

$$2C_{10}(r_\parallel + r_\perp) = \frac{2}{3}\frac{A_{\rm FB}\Gamma_f}{\mathcal{F}_\perp \mathcal{F}_\parallel}. \tag{A3}$$

We can write

$$\frac{F_\parallel F_\perp \Gamma_f^2}{4\mathcal{F}_\parallel^2 \mathcal{F}_\perp^2} = (r_\parallel r_\perp - C_{10}^2)^2 + C_{10}^2 (r_\parallel + r_\perp)^2$$
$$= (r_\parallel r_\perp - C_{10}^2)^2 + \frac{A_{\rm FB}^2 \Gamma_f^2}{9\mathcal{F}_\parallel^2 \mathcal{F}_\perp^2}$$

hence,

$$r_\parallel r_\perp - C_{10}^2 = \pm \frac{\Gamma_f}{2\mathcal{F}_\parallel \mathcal{F}_\perp}\sqrt{F_\parallel F_\perp - \frac{4A_{\rm FB}^2}{9}}. \tag{A4}$$

Now we can express C_{10}^2 in terms of $r_\parallel^2$ using Eq. (A1) or in terms of $r_\perp^2$ using Eq. (A2), to reexpress $r_\parallel r_\perp - C_{10}^2$:

$$2r_\parallel r_\perp - 2C_{10}^2 = 2r_\parallel r_\perp - \left(\frac{F_\parallel \Gamma_f}{2\mathcal{F}_\parallel^2} - r_\parallel^2\right) - \left(\frac{F_\perp \Gamma_f}{2\mathcal{F}_\perp^2} - r_\perp^2\right)$$
$$= \left[(r_\parallel + r_\perp)^2 - \frac{F_\parallel \Gamma_f}{2\mathcal{F}_\parallel^2} - \frac{F_\perp \Gamma_f}{2\mathcal{F}_\perp^2}\right]. \tag{A5}$$

Equating Eqs. (A4) and (A5) we get

$$r_\parallel + r_\perp = \pm\left[\frac{F_\parallel \Gamma_f}{2\mathcal{F}_\parallel^2} + \frac{F_\perp \Gamma_f}{2\mathcal{F}_\perp^2} \pm \frac{\Gamma_f}{2\mathcal{F}_\parallel \mathcal{F}_\perp} Z_1\right]^{1/2}$$
$$= \frac{\pm\sqrt{\Gamma_f}}{\sqrt{2}\mathcal{F}_\perp}[\mathsf{P}_1^2 F_\parallel + F_\perp \pm \mathsf{P}_1 Z_1]^{1/2}, \tag{A6}$$

where $Z_1 = \sqrt{4F_\parallel F_\perp - \frac{16}{9}A_{\rm FB}^2}$. Now, Eqs. (A1) and (A2) imply

$$r_\parallel^2 - r_\perp^2 = \frac{F_\parallel \Gamma_f}{2\mathcal{F}_\parallel^2} - \frac{F_\perp \Gamma_f}{2\mathcal{F}_\perp^2}, \tag{A7}$$

which gives $r_\parallel - r_\perp$ to be

$$r_\parallel - r_\perp = \frac{\pm\sqrt{\Gamma_f}}{\sqrt{2}\mathcal{F}_\perp}\frac{\mathsf{P}_1^2 F_\parallel - F_\perp}{[\mathsf{P}_1^2 F_\parallel + F_\perp \pm \mathsf{P}_1 Z_1]^{1/2}}. \tag{A8}$$

C_{10} is readily solved using Eq. (A3) and the expression for $r_\parallel + r_\perp$ obtained above. C_7 and C_9 are also easily solved using Eq. (23) and the expressions for $r_\parallel - r_\perp$. The solutions for C_7, C_9 and C_{10} are presented in Eqs. (47), (46), and (42), respectively.

APPENDIX B: FORM FACTOR CALCULATIONS

In this appendix we discuss the calculations of form factors and the form factor ratios. In our numerical analysis we have calculated the average value of the form factor $\mathcal{F}_\parallel$ and the two form factor ratios P_1 and P_1' in different q^2 regions.

As already discussed in Sec. IVA, at large recoil region the heavy quark symmetry applies and the seven form factors V, $A_{1,2,3}$, $T_{1,2,3}$ are functions of Isgur-Wise form factors $\xi_\parallel(q^2)$ and $\xi_\perp(q^2)$ [39]. These two form factors are parametrized as [15]

$$\xi_\perp(q^2) = \xi_\perp(0)\left(\frac{1}{1 - q^2/m_B^2}\right)^2,$$
$$\xi_\parallel(q^2) = \xi_\parallel(0)\left(\frac{1}{1 - q^2/m_B^2}\right)^3,$$

where $\xi_\perp(0) = 0.266 \pm 0.032$ and $\xi_\parallel(0) = 0.118 \pm 0.008$ [3]. The two ratios P_1, P_1' [see Eqs. (33a) and (33b)] are independent of Isgur-Wise form factors, and only $\mathcal{F}_\parallel$ [see Eq. (21)] is dependent on $\xi_\perp$. In Table III we have calculated the values of P_1, P_1' and $\mathcal{F}_\parallel$ averaged over each q^2 bin used by the recent experiments [10].

At low recoil the seven form factors V, $A_{1,2,3}$, $T_{1,2,3}$ are parametrized [40] as

$$\begin{aligned}
V(q^2) &= \frac{r_1}{1 - q^2/m_R^2} + \frac{r_2}{1 - q^2/m_{\rm fit}^2},\\
A_1(q^2) &= \frac{r_2}{1 - q^2/m_{\rm fit}^2},\\
A_2(q^2) &= \frac{r_1}{1 - q^2/m_{\rm fit}^2} + \frac{r_2}{(1 - q^2/m_{\rm fit}^2)^2},\\
T_1(q^2) &= \frac{r - 1}{1 - q^2/m_R 62} + \frac{r_2}{1 - q^2/m_{\rm fit}^2)^2},\\
T_2(q^2) &= \frac{r_2}{1 - q^2/m_{\rm fit}^2)^2},\\
T_3(q^2) &= \frac{m_B^2 - m_{K^*}}{q^2}(\tilde{T}_3(q^2) - T_2(q^2)),
\end{aligned} \tag{B1}$$

where $\tilde{T}_3$ has same parametrization as A_1. The parameters r_1, r_2, m_R^2, $m_{\rm fit}^2$ for each of the above form factors have been taken from Ref. [40]. Following the above parametrization, the ratios P_1, P_1' and $\mathcal{F}_\parallel$ have been calculated in the low-recoil region, averaged over each q^2 bin and have been shown in Table IV.

[1] R. Sinha, arXiv:hep-ph/9608314.
[2] F. Kruger, L. M. Sehgal, N. Sinha, and R. Sinha, Phys. Rev. D **61**, 114028 (2000).
[3] W. Altmannshofer, P. Ball, A. Bharucha, A. J. Buras, D. M. Straub, and M. Wick, J. High Energy Phys.01 (2009) 019.
[4] J. T. Wei *et al.* (BELLE Collaboration), Phys. Rev. Lett. **103**, 171801 (2009).
[5] B. Aubert *et al.* (*BABAR* Collaboration), Phys. Rev. D **79**, 031102 (2009).
[6] B. Aubert *et al.* (*BABAR* Collaboration), Phys. Rev. D **73**, 092001 (2006).
[7] CDF Public Note Report No. 10047.
[8] T. Aaltonen *et al.* (CDF Collaboration), Phys. Rev. Lett. **107**, 201802 (2011).
[9] T. Aaltonen *et al.* (CDF Collaboration), Phys. Rev. Lett. **108**, 081807 (2012).
[10] R. Aaij *et al.*, Phys. Rev. Lett. **108**, 181806 (2012).
[11] D. Das and R. Sinha, arXiv:1202.5105.
[12] G. Buchalla, A. J. Buras, and M. E. Lautenbacher, Rev. Mod. Phys. **68**, 1125 (1996).
[13] A. J. Buras, M. Misiak, M. Munz, and S. Pokorski, Nucl. Phys. **B424**, 374 (1994).
[14] A. J. Buras and M. Munz, Phys. Rev. D **52**, 186 (1995).
[15] M. Beneke, T. Feldmann, and D. Seidel, Nucl. Phys. **B612**, 25 (2001).
[16] Rare beauty and charm decays at LHCb, by C. Parkinson, 47th Rencontres de Moriond on QCD and High Energy Interactions, La Thuile, Italy, 2012, Report No LHCb-TALK-2012-040.
[17] P. Ball and V. M. Braun, Phys. Rev. D **58**, 094016 (1998); P. Ball and R. Zwicky, Phys. Rev. D **71**, 014029 (2005).
[18] V. L. Chernyak and A. R. Zhitnitsky, Pis'ma Zh. Eksp. Teor. Fiz. **25**, 544 (1977) [JETP Lett. **25**, 510 (1977)]; Yad. Fiz. **31**, 1053 (1980) [Sov. J. Nucl. Phys. **31**, 544 (1980)]; A. V. Efremov and A. V. Radyushkin, Phys. Lett. **94B**, 245 (1980); Teor. Mat. Fiz. **42**, 147 (1980) [Theor. Math. Phys. **42**, 97 (1980)]; G. P. Lepage and S. J. Brodsky, Phys. Lett. **87B**, 359 (1979); Phys. Rev. D **22**, 2157 (1980); V. L. Chernyak, A. R. Zhitnitsky, and V. G. Serbo, Pis'ma Zh. Eksp. Teor. Fiz. **26**, 760 (1977) [JETP Lett. **26**, 594 (1977)] Yad. Fiz. **31**, 1069 (1980)] [Sov. J. Nucl. Phys. **31**, 552 (1980).
[19] P. Colangelo and A. Khodjamirian, in *At the Frontier of Particle Physics*, edited by M. Shifman (World Scientific, Singapore, 2001), Vol. 3, pp. 1495–1576; A. Khodjamirian, AIP Conf. Proc. **602**, 194 (2001).
[20] A. Ali, P. Ball, L. T. Handoko, and G. Hiller, Phys. Rev. D **61**, 074024 (2000).
[21] C. Bobeth, G. Hiller, and G. Piranishvili, J. High Energy Phys. 07 (2008) 106.
[22] U. Egede, T. Hurth, J. Matias, M. Ramon, and W. Reece, J. High Energy Phys. 11 (2008) 032; J. Matias, F. Mescia, M. Ramon, and J. Virto, J. High Energy Phys. 04 (2012) 104.
[23] M. Beneke, G. Buchalla, M. Neubert, and C. T. Sachrajda, Phys. Rev. Lett. **83**, 1914 (1999).
[24] M. Beneke, G. Buchalla, M. Neubert, and C. T. Sachrajda, Nucl. Phys. **B591**, 313 (2000).
[25] C. W. Bauer, S. Fleming, and M. E. Luke, Phys. Rev. D **63**, 014006 (2000).
[26] C. W. Bauer, S. Fleming, D. Pirjol, and I. W. Stewart, Phys. Rev. D **63**, 114020 (2001).
[27] C. W. Bauer and I. W. Stewart, Phys. Lett. B **516**, 134 (2001).
[28] M. Beneke, A. P. Chapovsky, M. Diehl, and T. Feldmann, Nucl. Phys. **B643**, 431 (2002).
[29] R. J. Hill and M. Neubert, Nucl. Phys. **B657**, 229 (2003).
[30] A. Ali, G. Kramer, and G. H. Zhu, Eur. Phys. J. C **47**, 625 (2006).
[31] B. Grinstein and D. Pirjol, Phys. Rev. D **70**, 114005 (2004).
[32] J. Charles, A. L. Yaouanc, L. Oliver, O. Pene, and J. C. Raynal, Phys. Rev. D **60**, 014001 (1999).
[33] M. Beneke and T. Feldmann, Nucl. Phys. **B592**, 3 (2001).
[34] F. Kruger and J. Matias, Phys. Rev. D **71**, 094009 (2005).
[35] C. Bobeth, G. Hiller, and D. van Dyk, J. High Energy Phys. 07 (2010) 098.
[36] A. Y. Korchin and V. A. Kovalchuk, Phys. Rev. D **82**, 034013 (2010).
[37] A. Y. Korchin and V. A. Kovalchuk, arXiv:1111.4093.
[38] U. Egede, T. Hurth, J. Matias, M. Ramon, and W. Reece, J. High Energy Phys. 10 (2010) 056.
[39] N. Isgur and M. B. Wise, Phys. Lett. B **232**, 113 (1989); **237**, 527 (1990)
[40] P. Ball and R. Zwicky, Phys. Rev. D **71**, 014015 (2005); **71**, 014029 (2005).